KTH Information and Communication Technology

Adaptive MIMO Systems with Channel State Information at Transmitter

JIN LIANG HUANG

PhD Thesis
Stockholm, Sweden 2009

TRITA-ICT-COS-0804
ISSN 1653-6347
ISRN KTH/COS/R-08/04-SE
ISBN 978-91-7415-188-6

KTH School of Information and
Communication Technology
SE-16440 Stockholm
SWEDEN

Akademisk avhandling som med tillstånd av Kungl Tekniska högskolan framlägges till offentlig granskning för avläggande av teknologie doktorsexamen i Elektronik och Datorsystem fredag den 30 jan 2009 klockan 14:00 i sal E, Forum IT-Universitetet, Kungl Tekniska.

© Jin Liang Huang, January 2009

Tryck: Universitetsservice US AB

Abstract

This dissertation presents adaptation techniques that can achieve high spectral efficiency for single user multiple-input multiple-output (MIMO) systems. Two types of adaptation techniques, adaptive modulation and adaptive power allocation, are employed to adapt the rate and the transmit power to fading channels. We start by investigating the adaptive modulation subject to a certain bit-error-ratio (BER) constraint, either instantaneous BER constraint or average BER constraint. The resulting average spectral efficiencies are obtained in closed-form expressions. It turns out that, by employing the average BER constraint, we can achieve the optimal average spectral efficiency at the cost of prohibitive computational complexity. On the other hand, instantaneous BER constraint leads to inferior performance with little computational complexity. In order to achieve comparable performance to the average BER constraint with limited complexity, a non-linear optimization method is proposed. To further enhance the average spectral efficiency, adaptive power allocation schemes are considered to adjust the transmit power across the temporal domain or the spatial domain, depending on the specific situation. Provided the closed-form expressions of the average spectral efficiency, the optimal MIMO coding scheme that offers the highest average spectral efficiency under the same circumstances can be identified. As we take into account the effect of imperfect channel estimation, the adaptation techniques are revised to tolerate interference introduced by the channel estimation errors. As a result, the degradation with respect to the average spectral efficiency is in proportion to signal-to-noise ratio (SNR).

In order to facilitate fast development and verification of the adaptation schemes proposed for various MIMO systems, a reconfigurable Link Layer Simulator (LiLaS) which accommodates a variety of wireless/wireline applications is designed in the environment of MATLAB/OCTAVE. The idea of the simulator is originated from Software Defined Radio (SDR) and evolved to suit Cognitive Radio (CR) applications. For the convenience of modification and reconfiguration, LiLaS is functionally divided into generic blocks and all blocks are parameterized.
Keywords: adaptive modulation, adaptive power allocation, average spectral efficiency, MIMO, BER.

Acknowledgement

It takes me by surprise that how quickly three and a half years have passed without even being noticed. This is not a long period of time, but I have received the most unforgettable and rewarding experiences during this journey. Although, at the beginning of the journey, destination was rather vague and imprecise, it became more tangible and accurate as explorations went on. I don't think I would be able to accomplish, or start this journey without my advisor, Docent Svante Signell. I would like to express my sincere gratitude to him for giving me an opportunity to be a PhD student at KTH and, more importantly, for his enlightening guidance and continuous support since day one. I really appreciate that he granted me an open and free working atmosphere so that I could explore the areas I am interested in. I would like to give my hearty thanks to my co-advisor, Docent Slimane Ben Slimane, for reviewing my papers and discussing with me whenever I am confused. I owe a debt of gratitude to my colleague, Jinfeng Du, for always giving me constructive suggestions and reminding me important problems I neglect.

I would like to express my special gratitude to Prof. Jens Zander for his unconditional support. It is my great pleasure to join in the Department of CoS and work in such a pleasant atmosphere. I owe many thanks to people in my previous Department ECS. I am sincerely thankful to Prof. Hannu Tenhunen, Prof. Lirong Zheng, Prof. Mohammed Ismail, Docent Ana Rusu, as well as my advisor, for bringing me into the RaMSiS group.

I gratefully acknowledge all my former and present colleagues in the CoS and ECS departments, for sharing their precious knowledge and experience with me, for introducing me nice beer and food. I am sorry I can not put down your names because there are so many of you.

Many thanks go to Ulla Eriksson, Irina Radulescu, Robert Rönngren, Agneta Herling, Robin Gehrke, and Lena Beronius, for assisting me in many practical issues. Göran Andersson deserves special acknowledgment for helping me solve those tedious integrals.

Also, I'm grateful to all my friends in Sweden. I can not imagine how my life would be like without them. I'm especially grateful to my parents and my girlfriend for their encouragement and unconditioned support in all my decisions.

With no less respect, I am grateful to my Licentiate opponent Prof. Anders Ahlén from Uppsala University, and PhD proposal opponent Dr. Sören Andersson

from Ericsson, for their profund insight and valuable suggestions that help me improve the work. Last, but not the least, I would like to express my sincere acknowledgment to Prof. Geir Øien from NTNU for taking the time to be my opponent, Prof. Mats Viberg from Chalmers, Dr. Sören Andersson from Ericsson Research, and Prof. Mikael Skoglund from KTH, for acting as my Ph.D. committee members.

Notation and used symbols

Throughout this thesis, the following notations will be used:

$\mathbf{x}$	bold face lower-case letters denote column vectors
$\mathbf{A}$	bold face upper-case letters denote matrices
$\mathbf{a}_i$	the ith column vector of $\mathbf{A}$
$[\mathbf{A}]_{ji}$, $\mathbf{A}_{ji}$	the (j,i)th element of $\mathbf{A}$
$\mathbf{I}$	the identity matrix
$(\cdot)^*$	the complex conjugate transpose (Hermitian)
$\overline{(\cdot)}$	the complex conjugate
$(\cdot)^T$	the transpose
$\|\mathbf{x}\|_2$, $\|\mathbf{x}\|$	the Euclidean norm of $\mathbf{x}$
$\|\mathbf{A}\|_F$	the Frobenius norm of $\mathbf{A}$,$\|\mathbf{A}\|_F^2 = \mathrm{tr}(\mathbf{A}\mathbf{A}^*)$
$\mathrm{vec}(\mathbf{A})$	the vectorization operator, vec stacks the columns of $\mathbf{A}$ into a vector, i.e. $\mathrm{vec}(\mathbf{A}) = \begin{bmatrix} \mathbf{a}_1 \\ \vdots \\ \mathbf{a}_n \end{bmatrix}$

$\mathbf{A}^{\dagger}$	the Moore-Penrose pseudoinverse of $\mathbf{A}$ If the columns of $\mathbf{A}$ are linearly independent, then $\mathbf{A}^{\dagger} = (\mathbf{A}^{*}\mathbf{A})^{-1}\mathbf{A}^{*}$
$\mathbf{A}^{-1}$	the inversion of a non-singular square matrix, $\mathbf{A}^{-1}\mathbf{A} = \mathbf{I}$
tr	the trace of matrix
$\mathcal{CN}(\mu, \sigma^2)$	the circularly symmetric complex Gaussian random variable with mean μ and variance σ^2.

Here follows a list of some commonly used symbols in the thesis:

N_t	the number of transmit antennas
N_r	the number of receive antennas
$N_{\min}$	$N_{\min} = \min\{N_t, N_r\}$
$N_{\max}$	$N_{\max} = \max\{N_t, N_r\}$
N_s	the number of sub-channels that are used to deliver data
P_T	the total transmit power
σ_n^2	the variance of Gaussian white noise
$\mathbf{H}_w$	the complex valued i.i.d. Rayleigh fading channel
ρ_{tx}	the spatial correlation coefficients at the transmitter
ρ_{rx}	the spatial correlation coefficients at the receiver
γ_0	the system SNR defined as $\gamma_0 = \dfrac{P_T T_s}{\sigma_n^2}$
T_s	symbol duration time
λ_i	the ith eigenvalue of $\mathbf{HH}^{*}$
T_k	the SNR thresholds for adaptive modulation

Abbreviations and Acronyms

MIMO	multiple input multiple output
SISO	single input single output
OFDM	orthogonal frequency division multiplexing
CSI	channel state information
CQI	channel quality indicator
CSIT	channel state information at transmitter
CSIR	channel state information at receiver
CRSE	continuous-rate spectral efficiency
DRSE	discrete-rate spectral efficiency
BER	bit-error-ratio
I-BER	instantaneous BER
A-BER	average BER
SNR	signal to noise ratio
SINR	signal to interference plus noise ratio
SVD	singular value decomposition
BF	beamforming
OSTBC	orthogonal space-time block coding
ZF	zero forcing
MMSE	minimum mean square error
LiLaS	link layer simulator
SDR-WB	software defined radio workBench
i.i.d.	independent and identically distributed
p.d.f.	probability density function
d.o.f.	degrees of freedom
FDD	frequency division duplex
TDD	time division duplex
TCI	truncated channel inversion
CI	channel inversion
TAS	transmit antenna selection

List of publications

Journal papers:

1. Jinliang Huang and Svante Signell, "On Spectral Efficiency of Low-Complexity Adaptive MIMO Systems in Rayleigh Fading Channel", to appear in, *IEEE Transactions on Wireless Communications.*

2. Jinliang Huang and Svante Signell, "On Performance of Adaptive Modulation in MIMO Systems Using Orthogonal Space-Time Block Codes", second submission to *IEEE Transactions on Vehicular Technology.*

3. Jinliang Huang and Svante Signell, "Asymptotic Performance of MMSE MIMO Systems Using Adaptive Modulation", submitted to *IEEE Communications Letters.*

Conference papers (reviewed):

1. Jinliang Huang and Svante Signell, "Adaptive Modulation and Power Allocation for OSTBC", to be submitted.

2. Jinliang Huang and Svante Signell, "Discrete Rate Spectral Efficiency Improvement by Scheme Switching for MIMO Systems", *IEEE ICC,* Beijing, May 2008.

3. Jinliang Huang and Svante Signell, "Discrete Rate Spectral Efficiency for Adaptive MIMO Systems", *IEEE ICASSP,* Las Vegas, Mar. 2008.

4. Jinliang Huang and Svante Signell, "Impact of Channel Estimation Error on Performance of Adaptive MIMO Systems", *IEEE ICASSP,* Las Vegas, Mar. 2008.

5. Svante Signell and Jinliang Huang. "A Simulation Environment for Multi-Antenna Software Defined Radio", *IEEE ICICS,* Singapore, Dec. 2007.

6. Jinliang Huang and Svante Signell, "The spectral efficiency of Adaptive MIMO Systems in 2x2 Spatial Correlated Rayleigh Fading Channel", *IEEE FGCN,* Korea, Dec. 2007.

7. Jinliang Huang and Svante Signell, "Adaptive MIMO Systems in 2x2 uncorrelated Rayleigh fading channel", *IEEE WCNC,* HongKong, Mar. 2007.

8. Svante Signell and Jinliang Huang, "A Matlab/Octave Simulation Workbench for Software Defined Radio", *IEEE NORCHIP,* Linköping, Sweden, Nov. 2006.

9. Jinliang Huang and Svante Signell, "A Novel Power Allocation Strategy for Finite Alphabet in MIMO Systems", *IEEE VTC,* Melbourne, May. 2006.

10. Jinliang Huang and Svante Signell, "The Application of Rate Adaptation with Finite Alphabet in MIMO-OFDM", *IEEE ICICS,* Bankok, Dec. 2005.

Conference papers (non-reviewed):

1. Jinliang Huang and Svante Signell, "A Comparison of Two Algorithms in MIMO-OFDM", *IEEE SSoCC,* Stockholm, Apr. 2005.

2. Jinliang Huang and Svante Signell, "On Diversity Order of Singular Value Decomposition", *IEEE SSoCC,* Gullmarsstrand, Sweden, 2007.

3. Jinliang Huang and Svante Signell, "On Performance of Adaptive Modulation Systems with Channel Estimation Errors", *IEEE SSoCC,* Södertuna, May 2008.

Appended papers:

- Paper I: Jinliang Huang and Svante Signell, "Discrete Rate Spectral Efficiency Improvement by Scheme Switching for MIMO Systems", *IEEE ICC,* Beijing, May 2008.

- Paper II: Jinliang Huang and Svante Signell, "Impact of Channel Estimation Error on Performance of Adaptive MIMO Systems", *IEEE ICASSP,* Las Vegas, Mar. 2008.

- Paper III: Jinliang Huang and Svante Signell, "Asymptotic Performance of MMSE MIMO Systems Using Adaptive Modulation", submitted to *IEEE Communications Letters.*

- Paper IV: Jinliang Huang and Svante Signell, "On Performance of Adaptive Modulation in MIMO Systems Using Orthogonal Space-Time Block Codes", second submission to *IEEE Transactions on Vehicular Technology.*

- Paper V: Jinliang Huang and Svante Signell, "Adaptive Modulation and Power Allocation for OSTBC", to be submitted.

Contents

List of Figures

List of Tables

Chapter 1

Introduction

1.1 Background

Multiple Antenna Systems

In point-to-point wireless links, multiple-input multiple-output (MIMO) systems that utilize multiple antennas at transmitters and receivers can considerably increase link capacity as well as link reliability compared to conventional single-input single-output (SISO) systems [1–8]. The advantages originate from the multiple spatial channels, which are provided by the multiple antennas together with the scattering environment surrounding the transmitters and the receivers.

A general block diagram of MIMO systems is illustrated in Figure 1.1, where *MIMO encoder* and *MIMO decoder* accommodate various MIMO coding/decoding schemes, such as singular value decompostion (SVD) and orthogonal space-time block coding (OSTBC). By applying different coding/decoding schemes, the self-interfering MIMO channel can be converted into a set of parallel sub-channels, over which separate data streams are transmitted.

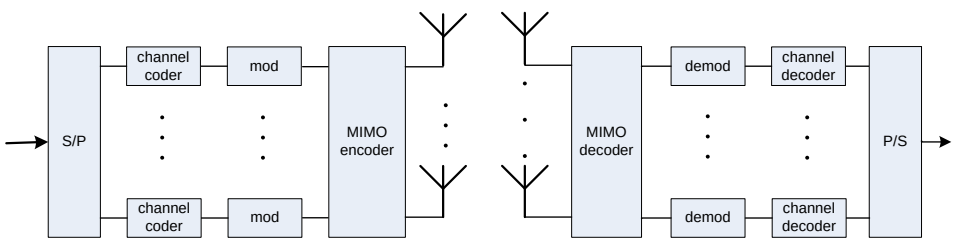

Figure 1.1: *Block diagram of MIMO systems.*

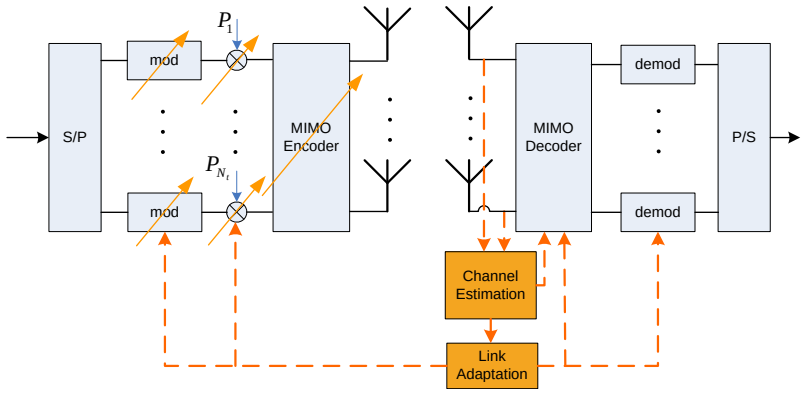

Figure 1.2: *Block diagram of MIMO systems with adaptive transmission.*

Channel-Adaptive Technologies

Adaptive transmission schemes that adjust transmission parameters with respect to time-varying channels enable robust and spectrally efficient communications. The essence of channel-adaptive transmission is to feedback channel state information (CSI) from receiver to transmitter so that the transmitter can adjust the parameters based on the feedback information with respect to the channel conditions. This technique was first investigated in [9], but it was shortly-lived maybe due to hardware constraints. Then it was re-visited in [10], where variable-rate, variable-power was suggested to approach channel capacity over Rayleigh fading channels. Thus far, adaptive transmission schemes have been applied to both SISO [10–13] and MIMO systems [14–27], and they mainly fall into three categories [21]:

- maximize the link spectral efficiency with fixed bit-error-ratio (BER) performance subject to a total power constraint [14–17, 19–21, 24],
- minimize BER with fixed rate subject to a total power constraint [21, 22, 29],
- minimize transmit power with fixed rate and fixed BER [23, 28].

In adaptive transmission technologies, the adaptation of parameters is based on the CSI, which can be either fed back to the transmitter in frequency division duplex (FDD) systems or can be estimated in the receiver mode in time division duplex (TDD) systems. A block diagram of adaptive transmission in FDD mode is shown in Figure 1.2, in which the receiver employs the link adaptation unit to determine the transmission parameters, and feed them back through a reverse channel.

1.2 State of The Art

The idea of adaptive power allocation and adaptive modulation was elaborated in [10] for SISO systems over Rayleigh fading channels. The impact of feedback delay was discussed and the maximum tolerable delay was provided. Later, it was concretized in [13] for adaptation in continuous-rate modulation order and discrete-rate modulation order, with either instantaneous BER (I-BER) constraint or average BER (A-BER) constraint. Furthermore, closed-form expressions were obtained for the average spectral efficiency, BER, and outage probability in [12]. Although the adaptation strategies proposed by [10, 12, 13] were oriented to SISO systems, [16] managed to extend it to MIMO SVD systems and tailored it to tolerate channel estimation errors. Moreover, the average spectral efficiency of MIMO SVD was obtained in the form of closed-form expression. Compared to the channel capacity and continuous-rate upper bound, the average spectral efficiency is an accurate estimation of the achievable spectral efficiency.

1.3 Outline and Contributions

Throughout this thesis, we consider adaptations based on FDD mode with error-free reverse channels from the receivers to the transmitters, thus the channel information at the transmitters is exactly the same as that at the receivers. Furthermore, we assume there is no evident feedback delay so that the adaptation decisions are never outdated. This is feasible in a relatively slowly fading channel where the coherence time is larger than the feedback delay. First and foremost, we consider adaptive modulation techniques targeting at maximizing spectral efficiency subject to BER and power constraints. The performance by using a number of MIMO coding schemes, e.g., SVD, beamforming (BF), OSTBC, spatial multiplexing with zero-forcing (ZF) receiver, spatial multiplexing with minimum-mean square error (MMSE) receiver, are evaluated. We obtain closed-form expressions of the average spectral efficiency, BER, and outage probability. The influence of imperfect channel estimation on performance is studied as well. We notice dramatic differences in the average spectral efficiencies that are achieved by applying different MIMO schemes, thereby it is beneficial to select the optimal MIMO coding scheme so as to achieve the highest possible average spectral efficiency. This turns out to be feasible thanks to the closed-form expressions, with which the average spectral efficiencies of all MIMO schemes can be calculated beforehand.

One important issue in adaptive modulation is the search for the SNR thresholds, which are used to choose the best-suited modulation order. By employing the Lagrangian method suggested in [13], we derive the optimal SNR thresholds for OSTBC that maximize the average spectral efficiency while meeting the A-BER constraint. In an attempt to reduce the complexity, a non-linear optimization algorithm is proposed to compute a set of sub-optimal SNR thresholds, which lead to comparable performance to that of the A-BER constraint. If we further relax

the assumption of constant transmit power and allow adaptive power allocation across time, as suggested in [13], considerable improvement on the average spectral efficiency can be acquired, especially in low SNR region.

It is known that, subject to the I-BER constraint and the peak power constraint, the optimal power allocation strategy for SVD is exhaustive search, which goes through every possible combination to find out the optimal choice on power and rate. In light of the intensive computational effort, we suggest another power control policy that can achieve comparable performance to the exhaustive search.

Last but not the least, we build up a generic and fully reconfigurable Link Layer Simulator (LiLaS) in the environment of MATLAB/OCTAVE, which supports various modulation and coding schemes, e.g., OFDM, MIMO, MIMO-OFDM, OFDM-OQAM, DS-CDMA.

Major contributions in this thesis are highlighted as follows:

1. obtained the closed-form expressions of the average spectral efficiencies for BF and SVD in 2×2 i.i.d. Rayleigh fading channels,
2. derived the closed-form expressions of the performance of MIMO OSTBC in doubly spatially correlated Rayleigh fading channels,
3. derived the closed-form expressions of the performance of MIMO ZF in semi-correlated Rayleigh fading channels,
4. obtained the closed-form expressions of the asymptotic performance of MIMO MMSE in i.i.d. Rayleigh fading channels,
5. evaluated the performance of adaptive modulation by imposing the I-BER constraint and the A-BER constraint in OSTBC systems,
6. suggested a method to calculate the sub-optimal SNR thresholds that lead to near-optimal average spectral efficiency while achieving near-target BER,
7. proposed selection of the optimal MIMO coding scheme based on the average spectral efficiency,
8. proposed the greedy power allocation that achieves near-optimal performance with much reduced computational complexity,
9. combined the adaptive modulation and adaptive power allocation in OSTBC systems,
10. developed the MATLAB/OCTAVE-based simulator, LiLaS.

Among them, $6, 7, 8$ are the unique contributions proposed by the author; contributions $1, 2, 3, 4, 5$ are based on the idea of adaptive modulation and the average spectral efficiency proposed by [10, 12, 13]; 9 is originated from the power allocation algorithm suggested for SISO [13]; 10 is evolved from Software Defined Radio Workbench (SDR-WB), which is a MATLAB/OCTAVE based simulator initially

developed by Svante Signell. This dissertation is organized into seven chapters. In more detail, the outline of each chapter is as follows:

Chapter 2 – MIMO Coding Schemes

We present the baseband signal model as well as the flat Rayleigh fading channel model for narrowband MIMO systems. Five MIMO coding schemes are briefly reviewed, namely SVD, BF, OSTBC, ZF, and MMSE.

Chapter 3 – Overview of Adaptive Modulation

In this chapter, a comprehensive review of adaptive modulation schemes is provided, including adaptive modulation for continuous-rate case and discrete-rate case. When discrete-rate modulation order is considered, the problem can be formulated as adaptive modulation with I-BER constraint or adaptive modulation with A-BER constraint. The algorithms for solving SNR thresholds subject to the I-BER constraint and the A-BER constraint are illustrated. The closed-form expressions of the average spectral efficiency, BER, and outage probability are derived.

Most of the material was encompassed in

> J. L. Huang and S. Signell, "On Performance of Adaptive Modulation in MIMO Systems Using Orthogonal Space-Time Block Codes", 2nd submission to *IEEE Transactions on Vehicular Technology*, December, 2008. (**Paper IV**)

Chapter 4 – Performance of Adaptive Modulation in MIMO Systems

This chapter presents the average spectral efficiencies by using adaptive modulation subject to I-BER constraint in various MIMO coding schemes, including SVD, BF, OSTBC, ZF, and MMSE. The average spectral efficiency of OSTBC under A-BER constraint is provided as well, which outperforms the one with I-BER constraint. Based on the performance of OSTBC under the I-BER constraint, a non-linear optimization method is introduced to achieve average spectral efficiency that is comparable to that of A-BER. Furthermore, the optimal MIMO coding scheme can be selected based on the average spectral efficiencies.

Most of the material was presented in

> Jinliang Huang and Svante Signell, "Adaptive MIMO Systems in 2×2 Uncorrelated Rayleigh Fading Channel," in *IEEE Proc. WCNC2007*, Hong Kong, Mar. 2007.
>
> Jinliang Huang and Svante Signell, "On Spectral Efficiency of Low-Complexity Adaptive MIMO Systems in Rayleigh Fading Channel," to appear in *IEEE Transactions on Wireless Communications.*

Jinliang Huang and Svante Signell, "Discrete rate spectral efficiency improvement by scheme switching for MIMO systems", in *IEEE Proc. ICC2008*, Beijing, May 2008. (**Paper I**)

Jinliang Huang and Svante Signell, "Asymptotic Performance of MMSE MIMO Systems Using Adaptive Modulation", submitted to *IEEE Communications Letters*. (**Paper III**)

Jinliang Huang and Svante Signell, "On Performance of Adaptive Modulation in MIMO Systems Using Orthogonal Space-Time Block Codes", 2nd submission to *IEEE Transactions on Vehicular Technology*, December, 2008. (**Paper IV**)

Chapter 5 – Adaptive Power Allocation for MIMO Systems

This chapter deals with adaptive power allocation for MIMO SVD and OSTBC systems. A practical power allocation scheme is suggested under the peak power constraint and the I-BER constraint for SVD, which exhibits near-optimal performance with considerably low computational complexity. In comparison to the average spectral efficiency of OSTBC without power adaptation, about 3dB gain can be achieved by applying adaptive power allocation when average power constraint and I-BER constraint are imposed.

Most of the material was included in

Jinliang Huang and Svante Signell, "A Novel Power Allocation Strategy for Finite Alphabet in MIMO Systems," in *Proc. IEEE VTC2006*, Melbourne, May, 2006.

Jinliang Huang and Svante Signell, "Adaptive Modulation and Power Allocation for OSTBC," to be submitted. (**Paper V**)

Chapter 6 – Adaptation Techniques with Imperfect Channel Estimation

The effects of channel estimation errors to adaptive modulation and adaptive power allocation are investigated in the context of MIMO OSTBC systems. Degradation of average spectral efficiency is unavoidable in order to tolerate the interferences caused by estimation errors.

The results can be found in

Jinliang Huang and Svante Signell, "Impact of Channel Estimation Error on Performance of Adaptive MIMO Systems", in *IEEE Proc. ICASSP2008*, Las Vegas, Mar. 2008. (**Paper II**)

Jinliang Huang and Svante Signell, "On Performance of Adaptive Modulation in MIMO Systems Using Orthogonal Space-Time Block Codes", 2nd submission to *IEEE Transactions on Vehicular Technology*, December, 2008. (**Paper IV**)

Jinliang Huang and Svante Signell, "Adaptive Modulation and Power Allocation for OSTBC," to be submitted. (**Paper V**)

Chapter 7 – Link Layer Simulator (LiLaS)

A short introduction of the reconfigurable simulator LiLaS is presented.
Part of the presentation was published in

Svante Signell and Jinliang Huang, "A Simulation Environment for Multi-Antenna Software Defined Radio", In *IEEE Proc. ICICS*, Singapore, Dec. 2007.

Appendices

Five selected papers are included in this part to complete the details that are not addressed in previous chapters. A brief introduction of these papers is outlined:

- **Paper I** addresses the adaptive modulation subject to the I-BER constraint in OSTBC and ZF systems. Closed-form expressions are obtained for the average spectral efficiency and BER.
- **Paper II** deals with the impact of channel estimation errors on the performance of adaptive modulation in OSTBC and ZF systems. The I-BER constraint is considered in both systems.
- **Paper III** evaluates the asymptotic performance of MIMO MMSE using adaptive modulation with the I-BER constraint.
- **Paper IV** extends the discussion from the I-BER constraint to the A-BER constraint. The optimal performance is obtained by applying A-BER constraint to OSTBC systems. A non-linear optimization method, the so-called LM algorithm, is employed to obtain a good trade-off between the performance and the complexity. The imperfect channel estimation is considered as well.
- **Paper V** utilizes both adaptive modulation and adaptive power allocation to OSTBC systems to improve the average spectral efficiency. The performance is also evaluated when imperfect channel estimation is considered.

For reading purpose, all papers included are reformatted to one-column with larger font size.

Chapter 2

MIMO Coding Schemes

2.1 Channel Model

A number of channel models for narrowband and wideband wireless links have been discussed in many works [36, 57–60] and [61] gives a complete review of the channel models. In our work, we employ a simple model proposed in [61, 62] to represent the narrowband wireless channel.

We consider a point-to-point MIMO system with N_t transmit antennas and N_r receive antennas in Rayleigh fading channels, where the channel can be modeled as

$$\mathbf{H} = \mathbf{R}_r^{1/2}\mathbf{H}_w\mathbf{R}_t^{1/2}. \tag{2.1}$$

$\mathbf{H}_w$ denotes the i.i.d. Rayleigh fading channel with no spatial correlation. Without loss of generality, the entries of $\mathbf{H}_w$ are assumed to be zero mean unit variance complex Gaussian random variables, i.e., $[\mathbf{H}_w]_{ij} \sim \mathcal{CN}(0,1)$. $\mathbf{R}_r$ and $\mathbf{R}_t$ represent the spatial correlations across the receiver antennas and transmitter antennas, respectively, which are modeled as:

$$[\mathbf{R}_r]_{ij} = \rho_{rx}^{|i-j|} \qquad \text{and} \qquad [\mathbf{R}_t]_{ij} = \rho_{tx}^{|i-j|},$$

where ρ_{rx} and ρ_{tx} are the correlation coefficients at the receiver and the transmitter, respectively, $0 \leq \rho \leq 1$. When there is no spatial correlation, $\rho_{rx} = \rho_{tx} = 0$ and the resultant channel matrix $\mathbf{H} = \mathbf{H}_w$. $\mathbf{R}_r^{1/2}$ and $\mathbf{R}_t^{1/2}$ are Hermitian matrices and can be decomposed as:

$$\mathbf{R}_r^{1/2} = \mathbf{U}_r\Lambda_r^{1/2}\mathbf{U}_r^*, \qquad \mathbf{R}_t = \mathbf{U}_t\Lambda_t^{1/2}\mathbf{U}_t^*,$$

where $\mathbf{U}_{r/t}$ is a unitary matrix and $\Lambda_{r/t}$ is a diagonal matrix with diagonal entries denoted by λ.

The channel is assumed to be quasi-static (channel coefficients remain constant during one time interval, and changes independently in the next interval). The

discrete-time baseband equivalent signal model can be written as:

$$\mathbf{y}(n) = \mathbf{H}(n)\mathbf{x}(n) + \mathbf{z}(n) \tag{2.2}$$

where $\mathbf{x}(n)$ is an $N_t \times 1$ transmitted vector and $\mathbf{y}(n)$ is an $N_r \times 1$ received vector. $\mathbf{z}(n)$ is the additive white Gaussian noise with covariance $\sigma_n^2 \mathbf{I}_{N_r \times N_r}$. The time index n is dropped in the following analysis for the purpose of simplicity.

We assume the total transmit power P_T is allocated across all non-zero entries of $\mathbf{x}$. Thus the energy of the transmitted vector is $E_s = P_T T_s$, where T_s is the symbol duration. If we assume a Nyquist data pulse, i.e., the utilized bandwidth $B = 1/T_s$, the average SNR can be defined as:

$$\gamma_0 = \frac{E_s}{\sigma_n^2}. \tag{2.3}$$

2.2 Overview of MIMO Coding Schemes

There exist a number of MIMO coding algorithms [64] and they can be classified as spatial multiplexing based schemes and diversity based schemes [35].

The spatial multiplexing schemes transmit separate streams of data across multiple antennas. At the receiver, there exist a variety of decoding techniques, e.g., joint maximum likelihood (ML) [30], sphere decoding [31], linear receiver with ZF detection [34], linear receiver with MMSE detection [34], successive interference cancellation (SIC) with ZF [34], SIC with MMSE[1] [34] and etc. Additionally, if precoding is feasible at the transmitter, SVD [36] can be adopted to convert the interfering MIMO channel into a set of parallel sub-channels, over which separate data streams are transmitted.

The diversity based schemes apply structured codes across space and time domain [4,5,32] to combine the diversity gains provided by the two dimensions. Alternatively, the codes can be employed across the space and frequency domain, such as space-frequency block code in MIMO-OFDM systems [33,55,56]. In narrowband systems, the most frequently used space-time codes are Alamouti codes [4] for two transmit antennas and generalized orthogonal space-time block codes for three or four transmit antennas [5].

In the following, we outline the fundamentals of the two classes of MIMO coding schemes, especially the effective SNR, which will play an important role in evaluating the performance of adaptive modulation in subsequent chapters.

Spatial Multiplexing Schemes

Singular Value Decomposition and Beamforming

The channel matrix $\mathbf{H}$ can be decomposed with the assistance of SVD:

$$\mathbf{H} = \mathbf{U}\Lambda\mathbf{V}^* \tag{2.4}$$

[1] this is also referred to as VBLAST.

where $\mathbf{U}$ and $\mathbf{V}$ are unitary matrices. Λ is an $N_r \times N_t$ matrix with $\{\sqrt{\lambda_1}, \ldots, \sqrt{\lambda_{N_{\min}}}\}$ on the diagonal and zeros otherwise. λ_i are the eigenvalues of $\mathbf{H}\mathbf{H}^*$ and $N_{\min} = \min\{N_t, N_r\}$.

By premultiplying with $\mathbf{V}$ at the transmitter and postmultiplying with $\mathbf{U}^*$ at the receiver, see (2.5), the channel is converted into a set of parallel sub-channels:

$$\hat{\mathbf{s}} = \mathbf{U}^*\mathbf{y} = \mathbf{U}^*\mathbf{H}\underbrace{\mathbf{V}\mathbf{s}}_{\mathbf{x}} + \tilde{\mathbf{z}} = \Lambda\mathbf{s} + \tilde{\mathbf{z}} \tag{2.5}$$

The effective SNR on the ith sub-channel is given as:

$$\gamma_i = \frac{\gamma_0 \lambda_i}{N_{\min}} \tag{2.6}$$

where γ_0 is the average SNR as defined above.

Beamforming is a special case of SVD, which utilizes only the strongest sub-channel and allocate all transmit power on it. The effective SNR is provided as:

$$\gamma = \gamma_0 \lambda_1 \tag{2.7}$$

Spatial Multiplexing with ZF Detection

We can write the channel matrix $\mathbf{H}$ (2.1) column-wisely:

$$\mathbf{H} = [\mathbf{h}_1, \mathbf{h}_2, \ldots, \mathbf{h}_{N_t}]$$

where $\mathbf{h}_i$ is the ith column of $\mathbf{H}$. Then the received signal can be rewritten as:

$$\mathbf{y} = \mathbf{h}_i x_i + \sum_{j \neq i} \mathbf{h}_j x_j + \mathbf{z} \tag{2.8}$$

which can be viewed as the sum of the desired signal x_i together with the interferences x_j and the noise. To extract x_i out of the received signal, $\mathbf{y}$ is projected onto a subspace orthogonal to the one spanned by the vectors $\mathbf{h}_1, \ldots, \mathbf{h}_{i-1}, \mathbf{h}_{i+1}, \ldots, \mathbf{h}_{N_t}$. The linear operation of the projection can be represented by a $d_i \times N_r$ matrix $\mathbf{Q}_i$, where d_i is found to be $N_r - N_t + 1$ [34]. The resulting signal after the projection is:

$$\tilde{\mathbf{y}}_i = \mathbf{Q}_i\mathbf{y} = \mathbf{Q}_i(\mathbf{h}_i x_i + \underbrace{\sum_{j \neq i} \mathbf{h}_j x_j + \mathbf{z}}_{\mathbf{w}_i}) \tag{2.9}$$

Then MRC is used to maximize the received SNR:

$$(\mathbf{Q}_i\mathbf{h}_i)^*\mathbf{Q}_i\mathbf{y}_i = \|\mathbf{Q}_i\mathbf{h}_i\|_2^2 x_i + (\mathbf{Q}_i\mathbf{h}_i)^*\mathbf{Q}_i\mathbf{w}_i \tag{2.10}$$

It can be proved that this method is equivalent to the least square solution, see Appendix 2.A,

$$\hat{\mathbf{x}} = \mathbf{H}^\dagger\mathbf{y} = (\mathbf{H}^*\mathbf{H})^{-1}\mathbf{H}^*\mathbf{y}, \tag{2.11}$$

for an over-determined system

$$\mathbf{y} = \mathbf{H}\mathbf{x}$$

where $\mathbf{H}$ is an $N_r \times N_t$ matrix with $N_r \geq N_t$.

The SNR of the ith stream can be obtained from (2.10)

$$\gamma_i = \frac{\gamma_0 \|\mathbf{Q}_i \mathbf{h}_i\|^2}{N_t}, \tag{2.12}$$

Spatial Multiplexing with MMSE Detection

The linear ZF receiver nulls out all inter-stream interferences at the cost of SNR degradation. Although it performs well in high SNR region, where the interferences dominate over additive Gaussian white noise, the performance is poor in low SNR region as the noise becomes the dominating factor. To take into account the noise, MMSE is the optimal linear filter that can maximize signal to interference plus noise ratio (SINR). The system model can be rewritten as:

$$\mathbf{y} = \mathbf{h}_i x_i + \underbrace{\sum_{j \neq i} \mathbf{h}_j x_j + \mathbf{z}}_{\mathbf{w}_i} \tag{2.13}$$

where $\mathbf{w}_i$ is viewed as colored noise with covariance matrix

$$\mathbf{K}_{w_i} = N_0 \mathbf{I} + \sum_{j \neq i} E_{s,j} \mathbf{h}_j \mathbf{h}_j^*,$$

where $E_{s,j}$ is the symbol energy on the jth transmit antenna. It is known that the maximal output SNR can be achieved by MRC if the noise is white. So a natural way is to prewhiten the noise:

$$\mathbf{K}_{w_i}^{-\frac{1}{2}} \mathbf{y} = \mathbf{K}_{w_i}^{-\frac{1}{2}} \mathbf{h}_i x_i + \mathbf{K}_{w_i}^{-\frac{1}{2}} \mathbf{w}_i, \tag{2.14}$$

and then project the output signal onto the direction along $\mathbf{K}_{w_i}^{-\frac{1}{2}} \mathbf{h}_i$:

$$\tilde{y}_i = (\mathbf{K}_{w_i}^{-\frac{1}{2}} \mathbf{h}_i)^* \mathbf{K}_{w_i}^{-\frac{1}{2}} \mathbf{y} = \mathbf{h}_i^* \mathbf{K}_{w_i}^{-1} \mathbf{y} = \mathbf{h}_i^* \mathbf{K}_{w_i}^{-1} \mathbf{h}_i x_i + \mathbf{h}_i^* \mathbf{K}_{w_i}^{-1} \mathbf{w}_i \tag{2.15}$$

The output SNR of the ith stream is

$$\gamma_i = E_{s,i} \mathbf{h}_i^* \mathbf{K}_{w_i}^{-1} \mathbf{h}_i \tag{2.16}$$

Then the decision statistic can be obtained by

$$\hat{x}_i = v_i \tilde{y}_i \tag{2.17}$$

where v_i can be solved from the MMSE method, which is formulated as:

$$v_i = \operatorname{argmin} \mathbf{E}\left[|x_i - \hat{x}_i|^2\right] \tag{2.18}$$

The minimum value could be achieved by

$$\frac{\partial \mathbf{E}\left[|x_i - \hat{x}_i|^2\right]}{\partial v_i} = 0, \tag{2.19}$$

which gives,

$$v_i = \frac{E_{s,i}}{1 + E_{s,i}\mathbf{h}_i^* \mathbf{K}_{w_i}^{-1} \mathbf{h}_i}, \tag{2.20}$$

and the resulting statistic is

$$\hat{x}_i = v_i \tilde{y}_i = \underbrace{\frac{E_{s,i}\mathbf{h}_i^* \mathbf{K}_{w_i}^{-1}}{1 + E_{s,i}\mathbf{h}_i^* \mathbf{K}_{w_i}^{-1} \mathbf{h}_i}}_{\mathbf{g}_i^*} \mathbf{y} \tag{2.21}$$

By stacking $\mathbf{g}_i^*$ for all transmit antennas, we arrive at the MMSE detection matrix[2]

$$\mathbf{G} = \begin{bmatrix} \mathbf{g}_1^* \\ \vdots \\ \mathbf{g}_{N_t}^* \end{bmatrix} = \mathbf{H}^* \left(N_0 \mathbf{I} + \mathbf{H}\mathbf{D}_E \mathbf{H}^*\right)^{-1} \tag{2.22}$$

where $\mathbf{D}_E$ is a diagonal matrix, $\mathrm{diag}(\mathbf{D}_E) = [E_{s,1}, \ldots, E_{s,n_t}]$, representing the symbol energy on each transmit antenna.

Observe that when the noise power is large enough, (2.22) degenerates to a matched filter:

$$\mathbf{G} = \mathbf{H}^* \left(N_0 \mathbf{I} + \mathbf{H}\mathbf{D}_E \mathbf{H}^*\right)^{-1} \approx \frac{1}{N_0} \mathbf{H}^*. \tag{2.23}$$

This is intuitively obvious since high noise power is the dominating factor and a matched filter can combine the signal power as much as possible so as to improve the SNR. In case of high SNR,

$$\mathbf{G} = \mathbf{H}^* \left(N_0 \mathbf{I} + \mathbf{H}\mathbf{D}_E \mathbf{H}^*\right)^{-1} \approx \mathbf{H}^* \left(\mathbf{H}\mathbf{D}_E \mathbf{H}^*\right)^{-1}. \tag{2.24}$$

If the total symbol energy E_s is equally assigned across the antennas, then $\mathbf{D}_E$ reduces to $\frac{E_s}{N_t}\mathbf{I}$ and (2.24) degenerates to the ZF method. Therefore, MMSE is a trade-off between the ZF detection and matched filtering.

Diversity Scheme

Orthogonal Space-Time Block Coding

Alamouti codes [4] is the most popular full diversity full rate OSTBC for two transmit antennas, in which the symbols to be transmitted are structured as a 2×2 block:

$$\begin{bmatrix} s_1 & -s_2^* \\ s_2 & s_1^* \end{bmatrix}.$$

[2] by using matrix inversion lemma: $(\mathbf{K} + \mathbf{h}\mathbf{h}^*)^{-1} = \mathbf{K}^{-1} - \frac{\mathbf{K}^{-1}\mathbf{h}\mathbf{h}^*\mathbf{K}^{-1}}{1+\mathbf{h}^*\mathbf{K}^{-1}\mathbf{h}}$

x^* represents the complex conjugate of x. The signals in the first row are the symbols to be transmitted through antenna 1 in two consecutive time slots, and the second row contains the data for antenna 2. The channel is assumed to be constant over two symbol intervals. As the number of transmit antennas increases, a group of half-rate and 3/4-rate orthogonal codes suggested by Tarokh V. *et al.* [5] are applicable. At the receivers, maximal-ratio combining (MRC) is employed to maximize the received SNR. In general, the effective SNR at the receiver can be written as:

$$\gamma = \frac{\gamma_0 \|\mathbf{H}\|_F^2}{RN_t}, \tag{2.25}$$

where $\|\cdot\|_F$ is the Frobenius norm, R is the OSTBC coding rate, γ_0 is average SNR as defined in (2.3). By substituting (2.1) into (2.25), the channel gain can be calculated as:

$$\|\mathbf{H}\|_F^2 = \mathrm{Tr}(\mathbf{H}\mathbf{H}^*) = \mathrm{Tr}(\mathbf{H}_w^* \Lambda_r \mathbf{H}_w \Lambda_t) = \sum_{i=1}^{N_r}\sum_{j=1}^{N_t} \lambda_{r,i}\lambda_{t,j}|[\mathbf{H}_w]_{ij}|^2, \tag{2.26}$$

which leads to an effective SNR:

$$\gamma = \frac{\gamma_0}{RN_t}\sum_{i=1}^{N_r}\sum_{j=1}^{N_t} \lambda_{r,i}\lambda_{t,j}|[\mathbf{H}_w]_{ij}|^2 = \sum_{i=1}^{N_r}\sum_{j=1}^{N_t}\gamma_{i,j}, \tag{2.27}$$

where $\gamma_{i,j} = \frac{\gamma_0}{RN_t}\lambda_{r,i}\lambda_{t,j}|[\mathbf{H}_w]_{ij}|^2$. From (2.27), the probability density function (p.d.f.) of γ can be obtained by using the moment-generating function (MGF). The approach is detailed in Paper IV.

2.3 Remarks

The principle of MIMO coding/decoding schemes is to transform the interfering MIMO channel into a set of parallel sub-channels, or one sub-channel (in the case of OSTBC), which does not interfere with each other. The transformations result in sub-channels with distinct statistical features, which essentially determine the overall performance of MIMO systems. With respect to adaptive modulation systems, the performance highly depends on the p.d.f. of the effective SNR of sub-channels, as will be shown in the next chapter.

Appendix

2.A Least square method for ZF

An over-determined system is written as:

$$\mathbf{y} = \mathbf{H}\mathbf{x} \tag{2.28}$$

where $\mathbf{H}$ is an $N_r \times N_t$ matrix with $N_r \geq N_t$. The least square method is to find an estimate $\hat{\mathbf{x}}$ that minimizes

$$\xi = \{\|\mathbf{y} - \mathbf{H}\hat{\mathbf{x}}\|^2\}. \tag{2.29}$$

This is solved by multiplying by a pseudoinverse matrix:

$$\hat{\mathbf{x}} = \mathbf{H}^{\dagger}\mathbf{y} = (\mathbf{H}^*\mathbf{H})^{-1}\mathbf{H}^*\mathbf{y} \tag{2.30}$$

In this appendix, it is shown that the pseudoinverse of $\mathbf{H}$ (2.30) is equivalent to the filter's solution in (2.10).

Without loss of generality, we look at the ith filter's coefficients:

$$\mathbf{c}_i^* = (\mathbf{Q}_i\mathbf{h}_i)^*\mathbf{Q}_i = \mathbf{h}_i^*\mathbf{Q}_i^*\mathbf{Q}_i, \tag{2.31}$$

where $\mathbf{Q}_i$ is composed of an orthonormal basis $\{\mathbf{q}_1^T, \mathbf{q}_2^T, \ldots, \mathbf{q}_{d_i}^T\}$, which spans the subspace $S^{\perp}$ that is orthogonal to the one spanned by the vectors

$$\{\mathbf{h}_1, \ldots, \mathbf{h}_{i-1}, \mathbf{h}_{i+1}, \ldots, \mathbf{h}_{N_t}\}.$$

Note that $\mathbf{Q}_i^*\mathbf{Q}_i$ is both hermitian and idempotent [39]: i.e. $(\mathbf{Q}_i^*\mathbf{Q}_i)^* = (\mathbf{Q}_i^*\mathbf{Q}_i)^2 = \mathbf{Q}_i^*\mathbf{Q}_i$, it can be viewed as a projection matrix onto subspace $S^{\perp}$, with the following properties:

1. $\mathbf{Q}_i^*\mathbf{Q}_i\mathbf{h}_i = \mathbf{h}_i$
2. $\mathbf{Q}_i^*\mathbf{Q}_i\mathbf{h}_j = 0$ where $j = 1, \ldots, i-1, i+1, \ldots, N_t$

By stacking the coefficients $\mathbf{c}_i^*$:

$$\mathbf{C} = \begin{bmatrix} \mathbf{h}_1^*\mathbf{Q}_1^*\mathbf{Q}_1 \\ \vdots \\ \mathbf{h}_{N_t}^*\mathbf{Q}_{N_t}^*\mathbf{Q}_{N_t} \end{bmatrix}$$

the product of $\mathbf{C}$ and $\mathbf{H}$ are:

$$\begin{aligned} \mathbf{CH} &= \begin{bmatrix} \mathbf{h}_1^*\mathbf{Q}_1^*\mathbf{Q}_1 \\ \vdots \\ \mathbf{h}_{N_t}^*\mathbf{Q}_{N_t}^*\mathbf{Q}_{N_t} \end{bmatrix} [\mathbf{h}_1, \cdots, \mathbf{h}_{N_t}] \\ &= \begin{bmatrix} \|\mathbf{h}_1\|^2 & \cdots & 0 \\ \vdots & \ddots & \vdots \\ 0 & \cdots & \|\mathbf{h}_{N_t}\|^2 \end{bmatrix} \end{aligned} \tag{2.32}$$

With properly chosen scaling factors for each row of $\mathbf{C}$, i.e. $1/\|\mathbf{h}_i\|^2$, we have $\mathbf{CH} = \mathbf{I}$ and hence

$$\mathbf{C} = \mathbf{H}^{\dagger}$$

Due to the uniqueness of pseudoinverse matrix,

$$\mathbf{C} = (\mathbf{H}^{*}\mathbf{H})^{-1}\mathbf{H}^{*}$$

Chapter 3

Overview of Adaptive Modulation

Adaptive modulation scheme aims to improve link spectral efficiency by adjusting the modulation order depending on the quality of fading channels. That is, more bits are transmitted when the channel quality is good and fewer bits are transmitted otherwise. In comparison to fixed modulation order strategy, this scheme is advantageous because it can achieve higher rate and more efficient use in the resources, e.g., time, frequency, and power. The mechanism of adaptive modulation is shown in Figure 3.1. The receiver estimates the channel-quality indicator (CQI) and feed it to the link adaptation, where the modulation order is selected based on CQI and eventually passed to the transmitter.

In this chapter, we will outline the adaptive modulation schemes for both continuous-rate modulation order and discrete-rate modulation order cases. Firstly, we will review adaptive modulation with continuous rate modulation order, namely the modulation order can take any nonnegative real value. Then we will look into

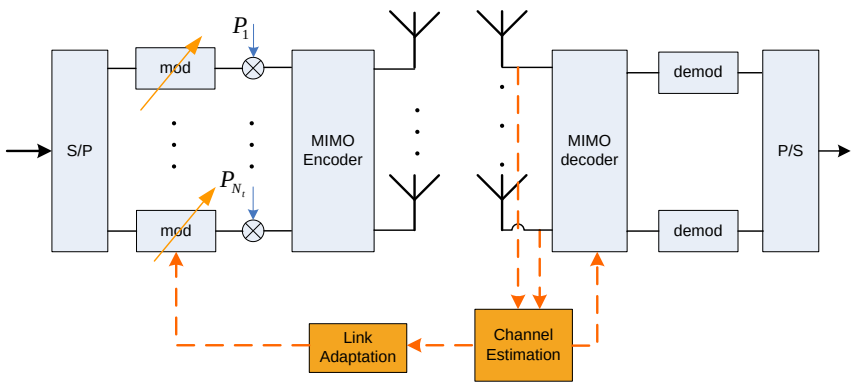

Figure 3.1: *Block diagram of adaptive modulation.*

the discrete rate case, where the modulation order is restricted to some certain integers. The reason for studying the continuous rate modulation is that it upper bounds the performance of practical modulation schemes and it is more analytically tractable due to rate continuity. In case of discrete-rate modulation order, a set of SNR thresholds have to be proposed that either fulfill I-BER constraint or A-BER constraint. In order to find the optimal SNR thresholds for the A-BER constraint, closed-form solutions for the average spectral efficiency and BER are needed. The study conducted herein is based on the assumption of fixed transmit power. Adaptive power allocation will be addressed later in Chapter 5.

3.1 Continuous-Rate Adaptive Modulation

In [10], the relationship of effective SNR (γ), error probability (P_b), and modulation order (M_k) of QAM modulation for coherent detection with Gray bit mapping is approximated as:

$$P_b \approx 0.2 \exp\left(-1.5 \frac{\gamma}{M_k - 1}\right), \tag{3.1}$$

which is tight within 1dB when $M_k \geq 4$ and $P_b \leq 10^{-3}$. Given (3.1), M_k can be rewritten as a function of P_b and γ. If we assume that the QAM symbols use a Nyquist data pulse, i.e., $B = 1/T_s$, then the continuous-rate spectral efficiency (CRSE) is equal to the average number of bits transmitted per channel use:

$$\text{CRSE} = \mathbf{E}\left\{\log M_k\right\} = \mathbf{E}\left\{\log(1 + g_o\gamma)\right\}, \tag{3.2}$$

where

$$g_o = \frac{-1.5}{\ln(5P_b)}$$

is the SNR gap [36, 37] between the CRSE and the Shannon capacity, which is incurred as infinite channel coding length and Gaussian signals are assumed in Shannon theory whereas uncoded QAM modulation is used herein.

When it comes to multi-antenna systems, the continuous-rate adaptive modulation scheme can be applied independently on each sub-channel and the resultant CRSE is:

$$\text{CRSE}_{\text{MIMO}} = \mathbf{E}\left\{\sum_{i=1}^{N_s} \log\left(1 + g_o\gamma_i\right)\right\}, \tag{3.3}$$

where N_s denotes the number of used sub-channels and γ_i is the effective SNR on the ith sub-channel. Recall the ergodic capacity of MIMO systems, an analogy can be drawn between the capacity and the CRSE, with the only difference caused by the SNR gap g_o.

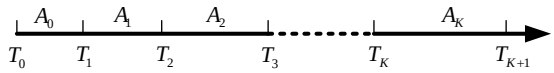

Figure 3.2: *Illustration of adaptive modulation.*

3.2 Discrete-Rate Adaptive Modulation

Now, we consider the situation in a real system where the modulation orders can only be drawn from a finite set of integers, e.g., $M_k = \{0, 1, 2, 4, 6 \ldots\}, k = 0 \ldots K$. The adaptive modulation divides the entire SNR region into $K + 1$ fading regions: $\mathcal{A}_k (k = 0, \ldots, K)$, one for each modulation order. Each fading region $\mathcal{A}_k$ is bounded by the associated SNR thresholds: $[T_k, T_{k+1})$, where T_k is the threshold that separates $\mathcal{A}_{k-1}$ and $\mathcal{A}_k$, as shown in Figure 3.2. The upper (T_{K+1}) and lower (T_0) limits of the thresholds are set to $+\infty$ and 0, respectively. Other SNR thresholds are to be solved to maximize spectral efficiency while satisfying certain constraints, depending on how the problem is formulated. Usually, there are two classes of constraints, BER constraints and power constraints. The power constraints will be elaborated in Chapter 5 and we restrict our discussions to the BER constraints in this chapter.

BER Constraints

In general, there exist two types of BER constraints: instantaneous BER (I-BER) constraint and average BER (A-BER) constraint. The instantaneous one requires that the error probability of every transmission is subject to the target level [13]:

$$P_b \leq \mathrm{BER}_t, \tag{3.4}$$

while the average constraint only cares about the average error probability after a large number of transmissions. That is, it relaxes the requirement on the instantaneous error probability and allows higher-than-target error probability at certain times:

$$\bar{P}_b \leq \mathrm{BER}_t \tag{3.5}$$

where BER_t is the predefined target BER, P_b and $\overline{P_b}$ are the instantaneous and average error probabilities, respectively. Obviously, the I-BER constraint is more restrictive than the A-BER constraint, so the corresponding spectral efficiency is certainly lower than the one subject to the A-BER constraint.

SNR Thresholds

When I-BER constraint is concerned, T_k should be set such that P_b in any time should be equal to or lower than the target. Thus, the SNR thresholds can be

obtained from (3.1) [10]:

$$T_k = \frac{M_k - 1}{1.5} \ln \frac{1}{5\text{BER}_t} \tag{3.6}$$

In this case, the resulting BER is guaranteed to be lower than the target, because, most of the time, the effective SNR is larger than T_k when modulation order M_k is selected. If we intend to hold the equality between P_b and BER_t, adaptive power allocation can be employed to maintain a constant effective SNR, which will be discussed further in Chapter 5.

In the case of A-BER constraint, SNR thresholds should be determined so as to maximize the average spectral efficiency while keeping the BER to the target level, i.e.,

$$\begin{cases} \max\limits_{T_1,\ldots,T_K} & \overline{\text{SE}}(T_1,\ldots,T_K) & \text{(3.7a)} \\ \text{subject to} & \bar{P}_b(T_1,\ldots,T_K) = \text{BER}_t & \text{(3.7b)} \end{cases}$$

where $\overline{\text{SE}}$ and $\overline{\text{BER}}$ are the analytical expressions of the average spectral efficiency and BER, respectively, which will be defined later. The optimal solutions for $\{T_1,\ldots,T_K\}$ could be found by utilizing the Lagrangian multipliers, by which the above constrained problem can be converted to an unconstrained optimization problem:

$$J(T_1,\ldots,T_K,\tau) = \overline{\text{SE}} - \tau(\bar{P}_b - \text{BER}_t), \tag{3.8}$$

where J is the Lagrangian. Then the optimal thresholds are determined by solving the following equations:

$$\begin{cases} \dfrac{\partial J(T_1,\ldots,T_K,\tau)}{\partial T_k} = 0, \quad \text{for} \quad \text{k=1,...,K} & \text{(3.9a)} \\ \dfrac{\partial J(T_1,\ldots,T_K,\tau)}{\partial \tau} = 0 & \text{(3.9b)} \end{cases}$$

To explore the optimal thresholds, analytical solutions for the average spectral efficiency and BER have to be found.

Average Spectral Efficiency

To be able to derive the optimal SNR thresholds as well as to evaluate the performance, it is necessary to obtain a closed-form expression for the average spectral efficiency. Since the modulation orders are in discrete form, the calculation can be made as follows [12]:

$$\overline{\text{SE}} = \sum_{i=1}^{N_s} \sum_{k=1}^{K} d_k \int_{T_k}^{T_{k+1}} p_{\gamma_i}(\gamma_i) d\gamma_i, \tag{3.10}$$

where $d_k = \log_2 M_k$ is the number of bits per symbol, N_s is the number of subchannels, $p_{\gamma_i}(\gamma_i)$ is the probability density function (p.d.f.) of γ_i on the ith subchannel. The average spectral efficiency is also referred to as discrete-rate spectral

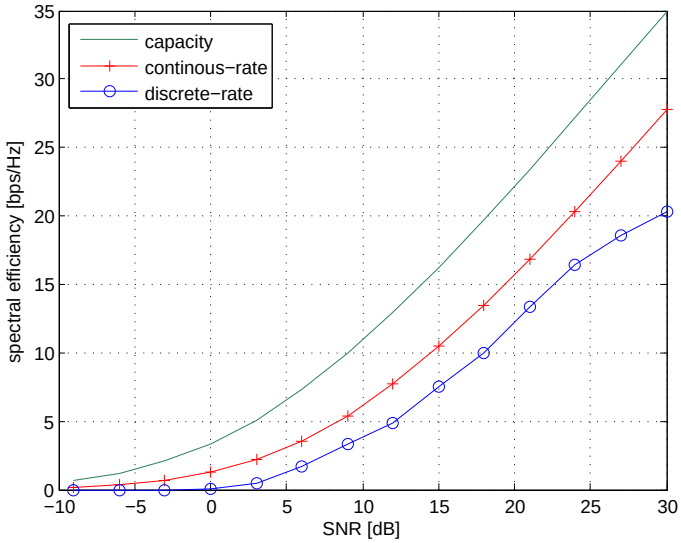

Figure 3.3: *A comparison of the capacity and the spectral efficiencies in 2×2 SVD systems.*

efficiency (DRSE) in Paper I, II, in contrast to the continuous-rate spectral efficiency. Figure 3.3 illustrates the differences among the capacity, the corresponding CRSE, and the average spectral efficiency/DRSE, in i.i.d. Rayleigh fading channels. The available modulation orders for MQAM modulation are assumed to be $\{0, 2, 4, 16, 64\}$. The SNR gap between the CRSE and the capacity is a constant that depends on the target BER only: $10\log_{10}\dfrac{-1.5}{\ln(5\mathrm{BER}_t)}$, which is about 5.5dB for a target BER of 0.1%. On the other hand, there exists an additional gap between the CRSE and the average spectral efficiency due to the discrete modulation order.

Approximation of BER

As suggested in [13], $\bar{P}_b$ can be computed as the ratio of average number of error bits and average number of bits:

$$\bar{P}_b = \frac{E\left[\text{number of error bits per transmission}\right]}{E\left[\text{number of bits per transmission}\right]} = \frac{\overline{\mathrm{NEB}}}{\overline{\mathrm{SE}}}, \tag{3.11}$$

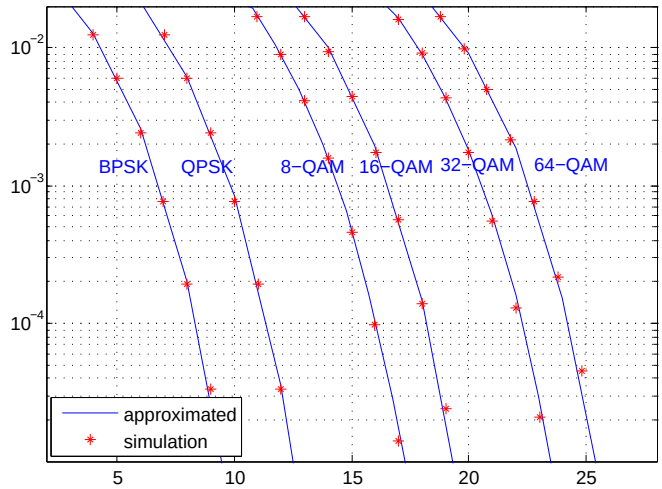

Figure 3.4: *Curve-fitting parameters for MQAM error probabilities in AWGN channels.*

mod	BPSK	QPSK	8-QAM	16-QAM	32-QAM	64-QAM
d_k	1	2	3	4	5	6
a_k	1.092	0.540	0.188	0.111	0.044	0.027
c_k	0.198	0.185	0.178	0.161	0.150	0.135

Table 3.1: *Curve-fitting for P_b with $BER_t = 10^{-3}$.*

where $\overline{\text{NEB}}$ can be approximated as:

$$\overline{\text{NEB}} \approx \sum_{i=1}^{N_s} \sum_{k=1}^{K} d_k \int_{T_k}^{T_{k+1}} P_b(\gamma_i) p_{\gamma_i}(\gamma_i) d\gamma_i \tag{3.12}$$

$P_b(\gamma_i)$ is the conditional error probability and it can be approximated by (3.1). However, the inaccuracy of (3.1) leads to noticeable errors in the resulting $\overline{P_b}$. Hence, a more precise approximation can be employed to each individual modulation order M_k:

$$P_b(\gamma, M_k) \approx c_k e^{-a_k \gamma}, \tag{3.13}$$

where a_k and c_k are parameters for specific modulation scheme, which can be found numerically by curve-fitting methods. As shown in Figure 3.4, the approximated P_b from (3.13) matches the simulation results, where the parameter values are tabulated in Table 3.1.

The key for solving the average spectral efficiency as well as the approximated $\bar{P}_b$ is the p.d.f. of the effective SNR, which is highly dependent on the channel characteristic, e.g., fading type and spatial correlation between the antennas at the transmitter/receiver. The p.d.f. of the effective SNR and the closed-form expressions described above will be mainly investigated in Chapter 4 for various MIMO coding schemes.

Provided the closed-form expressions of average spectral efficiency and $\bar{P}_b$, the optimal SNR thresholds suggested in (3.8) for the A-BER constraint can be solved. Unfortunately, there are no closed-form solutions and merely numerical solutions are available. Elaborated application of this method is discussed in Paper IV, where it was used to compute the optimal SNR thresholds for OSTBC.

Outage Probability

When wireless channel is null or in deep fades, the transmitted signal would be seriously attenuated and hence submerged by the noise. In order to use the resource in a more efficient way, transmission is only allowed when the channel is not in deep fades. The outage probability, in the context of discrete-rate modulation, is defined as the probability that the effective SNR falls below the lowest SNR threshold, T_1. In case there are N_s sub-channels, outage occurs only when every sub-channel is in outage and the outage probability can be calculated as the product of outage probability of each sub-channel:

$$P_{outage} = \prod_{i=1}^{N_s} \int_0^{T_1} p_{\gamma_i}(\gamma_i) d\gamma_i \tag{3.14}$$

Revisit of the A-BER Constraint

As has been shown in preceding sections, the exploration of SNR thresholds in the case of A-BER constraint entails the closed-form expressions of average spectral efficiency and $\bar{P}_b$. From the expressions given in (3.10) and (3.11), the optimization problem stated in (3.9a-3.9b) can be simplified to:

$$\begin{cases} C\Delta d_k = d_k c_k e^{-a_k T_k} - d_{k-1} c_{k-1} e^{-a_{k-1} T_k}, \qquad \text{for} \qquad \text{k=1,...,K} & \text{(3.15a)} \\ \dfrac{\overline{\text{NEB}}}{\overline{\text{SE}}} = \text{BER}_t & \text{(3.15b)} \\ \overline{\text{SE}} = \tau C - \tau \text{BER}_t & \text{(3.15c)} \end{cases}$$

where C is an unknown constant introduced to simplify the calculations, $\Delta d_k = d_k - d_{k-1}$. Note that (3.15a) corresponds to (3.9a), and (3.15b) imposes the BER constraint as in (3.9b). It is worth mentioning that τ is not of interest and it only appears in (3.15c), thereby it is sufficient to solve (3.15a) and (3.15b) in searching for the optimal SNR thresholds. When $k = 1$, $d_0 = 0$ and T_1 can be solved from

(3.15a)

$$T_1 = \frac{1}{a_1} \ln \frac{c_1}{C}. \tag{3.16}$$

The rest of T_k ($k > 1$) can be solved recursively. Although there are no closed-form solutions for the thresholds, numerical results are still feasible. An application of this algorithm can be found in Paper IV, in which the optimal SNR thresholds for OSTBC were solved by using this approach.

3.3 Remarks

The most important issue in applying practical adaptive modulation is the derivation of the SNR thresholds. It is trivial work to obtain the thresholds for the case of I-BER constraint. The obtained thresholds are independent of the average SNR γ_0, namely the same thresholds are used under all circumstances. However, the simplicity comes at the price of the average spectral efficiency: the achievable average spectral efficiency is always lower than the optimal one. On the other hand, the optimal average spectral efficiency can be obtained by imposing the A-BER constraint. The most obvious drawback of this method is, however, the complexity: numerical search has to be employed to find the optimal SNR thresholds for every specific SNR point, γ_0. Imaginably, numerous calculations have to be done and a high volume of data has to be stored. To find a good trade-off between these two occasions, a non-linear optimization algorithm will be introduced in the next chapter, to find one set of SNR thresholds that are applicable to the entire SNR region.

Chapter 4

Performance of Adaptive Modulation in MIMO Systems

In this chapter, we continue the discussion of adaptive modulation and apply the closed-form expressions (3.10,3.11,3.14) suggested in the preceding chapter to evaluate the performance of MIMO systems using various coding schemes, such as SVD, beamforming, OSTBC, ZF, and MMSE. The performance of adaptive modulation subject to instantaneous BER and average BER constraints are investigated, in which the optimal SNR thresholds for the A-BER constraint are determined and the maximal average spectral efficiency is obtained. To save computational effort of the optimal method, a nonlinear optimization method that can achieve comparable performance to the optimal one is introduced. Based on the average spectral efficiency, a MIMO scheme switching method is proposed to select the optimal coding scheme that achieves the highest spectral efficiency. Perfect CSI and ideal feedback is assumed in this chapter. That is, both transmitter and receiver have access to perfect CSI without any delay. The effects of channel estimation errors will be studied in Chapter 6.

4.1 I-BER Constraint

I-BER constraint can guarantee the error probability of every transmission is lower than the target BER. Based on this condition, the SNR thresholds are determined by rewriting (3.13):

$$T_k = \frac{1}{a_k} \ln \frac{c_k}{\mathrm{BER}_t}, \tag{4.1}$$

where a_k and c_k can be drawn from Table 3.1 for specific modulation order, if BER_t is set to be 0.1%. Provided the SNR thresholds, the average spectral efficiency is derived as:

$$\overline{\mathrm{SE}} = \sum_{i=1}^{N_s} \sum_{k=1}^{K} d_k \int_{T_k}^{T_{k+1}} p_{\gamma_i}(\gamma_i) d\gamma_i, \tag{4.2}$$

where the major problem is determination of the p.d.f. of the effective SNR, $p_{\gamma_i}(\gamma_i)$.

SVD and Beamforming

In 2×2 i.i.d. Rayleigh fading channels, SVD creates two independent eigenvalue sub-channels. The p.d.f. of the effective SNR in every sub-channel can be computed as:

$$p_{\gamma_1}(\gamma_1) = \left(\frac{8\gamma_1^2}{\gamma_0^3} - \frac{8\gamma_1}{\gamma_0^2} + \frac{4}{\gamma_0}\right) e^{-\frac{2\gamma_1}{\gamma_0}} - \frac{4}{\gamma_0} e^{-\frac{4\gamma_1}{\gamma_0}} \tag{4.3}$$

$$p_{\gamma_2}(\gamma_2) = \frac{4}{\gamma_0} e^{-\frac{4\gamma_2}{\gamma_0}} \tag{4.4}$$

By inserting the p.d.f. into (4.2), we get the average spectral efficiency of SVD with equal power allocation as a function of γ_0:

$$\overline{\mathrm{SE}}_{svd}(\gamma_0) = \sum_{k=1}^{K} \Delta d_k e^{\frac{-2T_k}{\gamma_0}} \left[\left(\frac{2T_k}{\gamma_0}\right)^2 + 2\right], \tag{4.5}$$

where $\Delta d_k = d_k - d_{k-1}$ and $d_0 = 0$. Similarly, we can derive the average spectral efficiency of beamforming by utilizing the strongest eigenvalue and allocate all transmit power onto the corresponding sub-channel:

$$\overline{\mathrm{SE}}_{bf}(\gamma_0) = \sum_{k=1}^{K} \Delta d_k e^{\frac{-T_k}{\gamma_0}} \left[\left(\frac{T_k}{\gamma_0}\right)^2 + 2 - e^{\frac{-T_k}{\gamma_0}}\right]. \tag{4.6}$$

The resulting average spectral efficiencies are plotted in Figure 4.1, where the modulation orders are selected from the set: $\{0, 2, 4, 16, 64\}$. It is observed that beamforming achieves higher spectral efficiency in low SNR region while SVD outperforms beamforming at high SNRs. This is intuitively true because power gain is favored in the low SNR region and spatial multiplexing gain is advantageous in the high SNR region, [73].

A more general form of the average spectral efficiency for arbitrary number of transmit and receive antennas is provdied in [16]. However, the generalized closed-form expressions are obtained based on the assumption of i.i.d. Rayleigh fading channels. The more complicated problem with spatially correlated Rayleigh fading channels has not been addressed yet.

ZF

We consider semi-correlated Rayleigh channels with spatial correlation at transmitters. The effective SNR on the ith stream of the ZF receiver follows a gamma distribution [40]:

$$p_{\gamma_i}(\gamma_i) = \frac{\sigma_i^2 e^{-\gamma_i \sigma_i^2 / \frac{\gamma_0}{N_t}}}{\frac{\gamma_0}{N_t}\Gamma(N_r - N_t + 1)} \left(\frac{\gamma_i \sigma_i^2}{\gamma_0 / N_t}\right)^{N_r - N_t}, \tag{4.7}$$

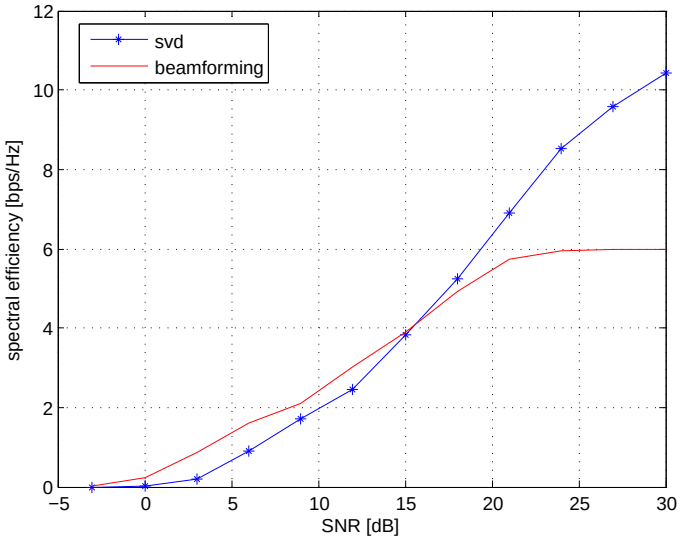

Figure 4.1: *Average spectral efficiencies of SVD and beamforming in* 2×2 *i.i.d. Rayleigh fading channels.*

where σ_i^2 is the ith diagonal entry of $\mathbf{R}_t^{-1}$, $\Gamma(N_r - N_t + 1) = (N_r - N_t)!$. The average spectral efficiency can be obtained as:

$$\overline{\mathrm{SE}}_{zf}(\gamma_0, \sigma_i^2) = \sum_{i=1}^{N_t} \sum_{k=1}^{K} \Delta d_k \frac{\Gamma_u(N_r - N_t + 1, \frac{\sigma_i^2 T_k}{\gamma_0 / N_t})}{\Gamma(N_r - N_t + 1)}, \tag{4.8}$$

where $\Gamma_u\big(a, x\big)$ is the upper incomplete Gamma function:

$$\Gamma_u\big(a, x\big) = \int_x^{\infty} t^{a-1} e^{-t} dt. \tag{4.9}$$

If the channel is spatially uncorrelated, $\rho_{tx} = 0$ and $\sigma_i^2 = 1$. The resulting average spectral efficiency is:

$$\overline{\mathrm{SE}}_{zf}(\gamma_0) = \sum_{i=1}^{N_t} \sum_{k=1}^{K} \Delta d_k \frac{\Gamma_u(N_r - N_t + 1, \frac{T_k}{\gamma_0 / N_t})}{\Gamma(N_r - N_t + 1)} \tag{4.10}$$

It has been shown in many works, e.g. [41], that capacity is subject to spatial correlations. As a result, the average spectral efficiency also depends on the spatial correlation. The impact of spatial correlation on spectral efficiency is shown in Figure 4.2, where $\rho_{tx} = 0.1, 0.5, 0.9$. The average spectral efficiency of ZF degrades

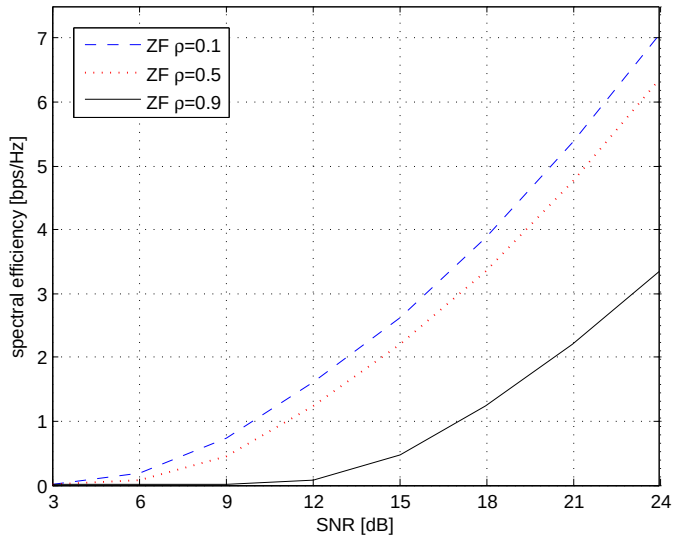

Figure 4.2: *Average spectral efficiencies of ZF in* 2×2 *spatially correlated Rayleigh fading channels.*

dramatically as ρ_{tx} increases. The idea of ZF is to project the received signal, consisting of two parts–the interference and the desired signal, onto a subspace that is orthogonal to the interference while keeping as much as possible of the desired signal. In presence of high spatial correlation at the transmitter, the interference is aligned in a direction close to the desired signal and the effective SNR would inevitably suffer from the projection.

MMSE

In [42], three types of distributions are proposed to approximate the p.d.f. of the effective signal-to-noise-and-interference ratio (SINR), namely Appr. A, Appr. B, and Appr. C. Appr. A treats the p.d.f. of SINR as a gamma distribution, $G(m, \theta)$. The p.d.f. of γ_i is characterized by m and θ:

$$f_g(\gamma_i) = \gamma_i^{m-1} \frac{e^{-\gamma_i/\theta}}{\theta^m \Gamma(m)}, \tag{4.11}$$

where the values of m and θ are provided in Paper III. In the context of i.i.d. Rayleigh fading channels, all sub-channels have the same distribution. The average

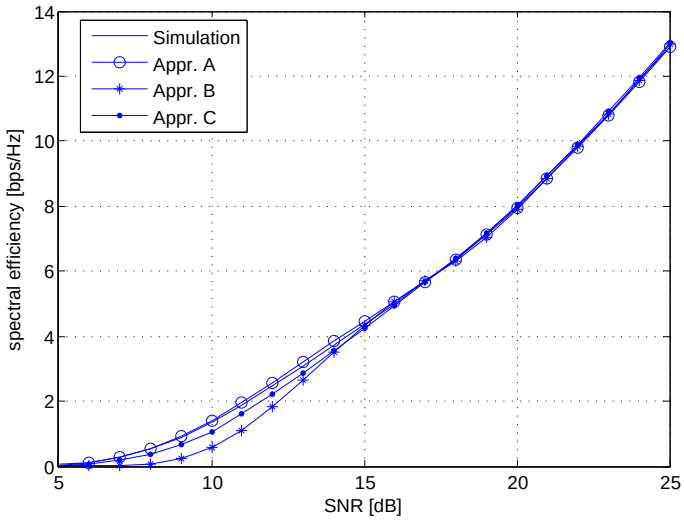

Figure 4.3: *Approximated average spectral efficiencies of MMSE in* 4×4 *i.i.d. Rayleigh fading channels.*

spectral efficiency is N_t times the average spectral efficiency of one sub-channel:

$$\overline{\mathrm{SE}}_g = N_t \sum_{k=1}^{K} \Delta d_k \frac{\Gamma_u\left(m, \frac{T_k}{\theta}\right)}{\Gamma(m)} \tag{4.12}$$

Moreover, Appr. B regards γ_i as generalized gamma distribution. Appr. C regards γ_i as a sum of two independent variables: one is gamma distributed and the other is generalized gamma distributed. Then the p.d.f. of γ_i is the convolution of gamma distribution and generalized gamma distribution [66]. The theoretical results based on the three approximations are compared to the actual result from simulation. It is observed that the first approximation generates the most accurate numerical results while Appr. B gives the worst performance. The discrepancies between the approximations and the real values are more noticeable in low SNR region.

OSTBC

In the case of OSTBC, we assume arbitrary number of antennas as well as arbitrary spatial correlation at the transmitter and the receiver. The generalized form of the p.d.f. of the effective SNR can be derived by using moment-generating function (MGF). The resulting p.d.f. can be classified into two cases: non repeated roots case and repeated roots case. Before elaborating on the two cases, let's define a

new parameter:

$$\alpha_{i,j} = \frac{\gamma_0 \lambda_{r,i} \lambda_{t,j}}{RN_t}, \tag{4.13}$$

where $\gamma_0 = E_s/\sigma_n^2$ is the average SNR as defined in (2.3), $\lambda_{r,i}$ and $\lambda_{t,j}$ represent the correlation at the receiver and the transmitter, respectively, which are the singular values of the correlation matrices. R is the coding rate for OSTBC, $R = 1$ for Alamouti code and $R = 1/2$ or $3/4$ for orthogonal codes with 3 or 4 transmit antennas. Given $\alpha_{i,j}$, $\gamma_{i,j} = \alpha_{i,j}|[\mathbf{H}_w]_{ij}|^2$ and the MGF of γ can be derived as:

$$M_\gamma(s) = \prod_{i=1}^{N_r} \prod_{j=1}^{N_t} \frac{1}{1 - \alpha_{i,j} s}, \tag{4.14}$$

Then the p.d.f. of the effective SNR can be obtained by inverse Laplace transform of $M_\gamma(-s)$. The repeated roots and non repeated roots refer to the multiplicity of roots $s = 1/\alpha_{i,j}$.

- Case I (non repeated roots): $\alpha_{i,j} = \alpha_{k,l}$ iff $k = i$ and $l = j$, namely, $\rho_{tx} \neq \rho_{rx}$ and $\rho_{tx}\rho_{rx} \neq 0$. This is the case of doubly-correlated fading channel with different correlation coefficients at the transmitter and the receiver.

$$p_\gamma(\gamma) = \sum_{i=1}^{N_r} \sum_{j=1}^{N_t} \frac{\varphi_{i,j}}{\alpha_{i,j}} e^{-\frac{\gamma}{\alpha_{i,j}}} \tag{4.15}$$

  where $\varphi_{i,j}$ can be obtained as follows:

$$\varphi_{i,j} = (1 - \alpha_{i,j} s) M_\gamma(s) \Big|_{s = 1/\alpha_{i,j}}. \tag{4.16}$$

  Detailed derivations of the p.d.f. from the MGF are included in Paper I.

- Case II (repeated roots): there exists $\alpha_{i,j} = \alpha_{k,l}$ when $k \neq i$ or $l \neq j$, i.e., $\rho_{tx}\rho_{rx} = 0$ or $\rho_{tx} = \rho_{rx}$. In other words, they correspond to the cases of non-correlated (i.i.d.) channel, semi-correlated channel, or doubly correlated channel with the same correlation coefficient. Let's assume that $\alpha_{i,j}$ have in total N_d different values, denoted by α_m, $m = 1, \ldots, N_d$, and each value repeats $N_s(m)$ times, $1 \leq N_s(m) \leq N_r N_t$. The MGF can be rewritten as

$$M_\gamma(s) = \prod_{m=1}^{N_d} \prod_{l=1}^{N_s(m)} \frac{1}{(1 - \alpha_m s)^l} = \sum_{m=1}^{N_d} \sum_{l=1}^{N_s(m)} \frac{\varphi_{m,l}}{(1 - \alpha_m s)^l}, \tag{4.17}$$

  where $\varphi_{m,l}$ can be calculated as follows:

$$\varphi_{m,l} = \frac{(-1/\alpha_m)^{N_s(m)-l}}{(N_s(m) - l)!} \frac{d^{N_s(m)-l}}{ds^{N_s(m)-l}} \left[(1 - \alpha_m s)^{N_s(m)} M_\gamma(s) \right] \Big|_{s = 1/\alpha_m} \tag{4.18}$$

With all coefficients set by the equation above, the p.d.f. of γ is obtained as:

$$p_\gamma(\gamma) = \sum_{m=1}^{N_d} \sum_{l=1}^{N_s(m)} \frac{\varphi_{m,l}\gamma^{l-1}}{\Gamma(l)\alpha_m^l} e^{-\frac{\gamma}{\alpha_m}}. \tag{4.19}$$

As the p.d.f. of the effective SNR is determined, the average spectral efficiency for case I can be calculated:

$$\overline{\mathrm{SE}}_{\mathrm{I}}(\gamma_0, \rho_{tx}, \rho_{rx}) = R \sum_{k=1}^{K} \sum_{i=1}^{N_r} \sum_{j=1}^{N_t} \varphi_{i,j} \Delta d_k e^{-\frac{T_k}{\alpha_{i,j}}}, \tag{4.20}$$

The average spectral efficiency for case II is:

$$\overline{\mathrm{SE}}_{\mathrm{II}}(\gamma_0, \rho_{tx}, \rho_{rx}) = R \sum_{k=1}^{K} \sum_{m=1}^{N_d} \sum_{l=1}^{N_s(m)} \frac{\varphi_{m,l}}{\Gamma(l)} \Delta d_k \Gamma_u\big(l, \frac{T_k}{\alpha_m}\big). \tag{4.21}$$

Figure 4.4 shows the average spectral efficiencies that can be achieved by using OSTBC when $N_t = N_r = 2, 3, 4$. Since half-rate orthogonal codes are employed when $N_t = 3$ and 4, the maximal achievable rates are only half of that achieved by Alamouti code. Figure 4.5 shows the impact of spatial correlation on the average spectral efficiency. Recall what has been shown in Figure 4.2, it is noticed that OSTBC is more robust to the variation of the spatial correlation compared to ZF. This is because the average spectral efficiency is essentially dominated by the channel gain, which experiences only small variation as the correlation changes.

Similarly, the BER can be obtained by inserting the p.d.f. into (3.11):

$$\bar{P}_{b,\mathrm{I}}(\gamma_0, \rho_{tx}, \rho_{rx}) \approx \frac{R}{\overline{\mathrm{SE}}_{\mathrm{I}}} \sum_{k=1}^{K} \sum_{i=1}^{N_r} \sum_{j=1}^{N_t} \frac{c_k d_k \varphi_{i,j}}{1 + a_k \alpha_{i,j}} \Psi_{\mathrm{I}}(k, i, j) \tag{4.22}$$

where

$$\Psi_{\mathrm{I}}(k, i, j) = e^{-(a_k + \frac{1}{\alpha_{i,j}})T_k} - e^{-(a_k + \frac{1}{\alpha_{i,j}})T_{k+1}}$$

$$\bar{P}_{b,\mathrm{II}}(\gamma_0, \rho_{tx}, \rho_{rx}) \approx \frac{R}{\overline{\mathrm{SE}}_{\mathrm{II}}} \sum_{k=1}^{K} \sum_{m=1}^{N_d} \sum_{l=1}^{N_s(m)} \frac{c_k d_k \varphi_{m,l}}{\Gamma(l)\,(1 + a_k \alpha_m)^l} \Psi_{\mathrm{II}}(k, m, l) \tag{4.23}$$

where

$$\Psi_{\mathrm{II}}(k, m, l) = \Gamma_u\left(l, T_k(a_k + \frac{1}{\alpha_m})\right) - \Gamma_u\left(l, T_{k+1}(a_k + \frac{1}{\alpha_m})\right)$$

The approximated BER according to (4.23) is compared with the actual BER obtained from computer simulation in Figure 4.6. The differences between the real BER and approximated BER are negligible. However, the resulting BER is always below the target BER, 0.1% in this case. In order to obtain a BER that is equal to

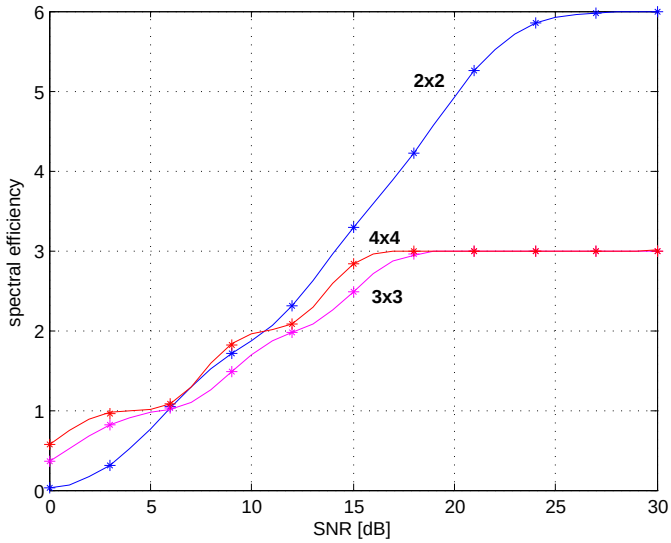

Figure 4.4: *Average spectral efficiencies of OSTBC in $N_r \times N_t$ spatially correlated Rayleigh fading channels, $\rho_{tx} = \rho_{rx} = 0.5$.*

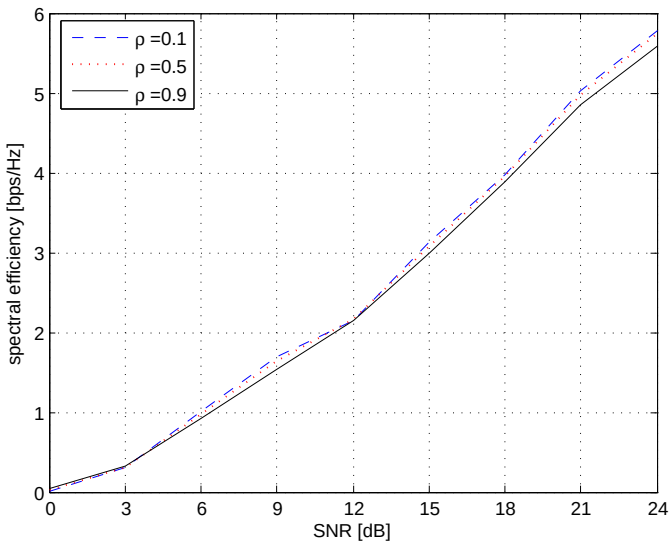

Figure 4.5: *Average spectral efficiencies of OSTBC in 2×2 spatially correlated Rayleigh fading channels, $\rho_{tx} = 0.1, 0.5, 0.9$, $\rho_{rx} = 0$.*

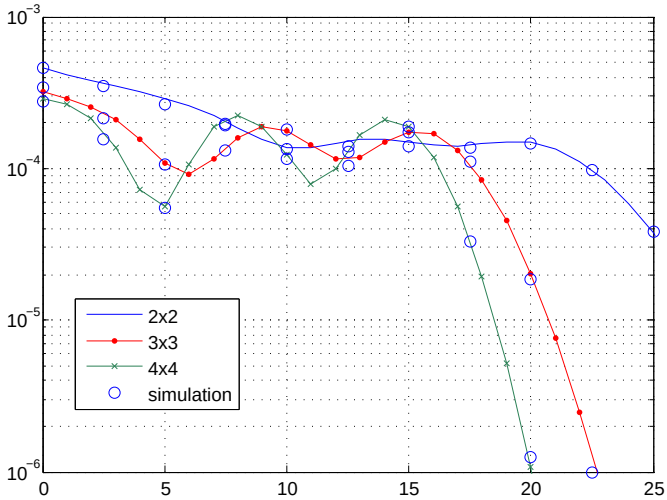

Figure 4.6: *BER performance of OSTBC in spatially correlated Rayleigh fading channels,* $\rho_{tx} = \rho_{rx} = 0.5$.

the prescribed target, lower SNR thresholds have to be found. This problem will be further studied in Section 4.3, where a non-linear optimization method can be used to adjust the SNR thresholds.

The outage probability is calculated as the probability that the effective SNR is lower that the first SNR threshold, T_1:

$$P_{outage,\mathrm{I}}(\gamma_0, \rho_{tx}, \rho_{rx}) = \sum_{i=1}^{N_r} \sum_{j=1}^{N_t} \varphi_{i,j} \left(1 - e^{-\frac{T_1}{\alpha_{i,j}}}\right), \tag{4.24}$$

$$P_{outage,\mathrm{II}}(\gamma_0, \rho_{tx}, \rho_{rx}) = \sum_{m=1}^{N_d} \sum_{l=1}^{N_s(m)} \frac{\varphi_{m,l}}{\Gamma(l)} \Gamma_l\left(l, \frac{T_1}{\alpha_m}\right) \tag{4.25}$$

where $\Gamma_l(a, x)$ is the lower incomplete gamma function defined as:

$$\Gamma_l(a, x) = \int_0^x t^{a-1} e^{-t} dt. \tag{4.26}$$

The outage probabilities for systems in deep fades are shown in Figure 4.7.

4.2 A-BER Constraint

Although the I-BER constraint can achieve a lower-than-target BER, as can be seen in Figure 4.6, this gain is actually obtained at the cost of spectral efficiency. In

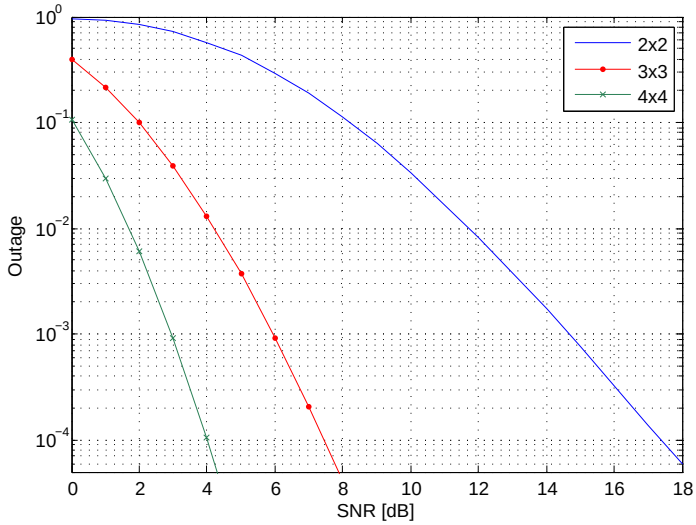

Figure 4.7: *Outage probability of OSTBC in spatially correlated Rayleigh fading channel,* $\rho_{tx} = \rho_{rx} = 0.5$.

other words, we can improve the average spectral efficiency if the SNR thresholds are delicately set such that the BER is equivalent to the target. Thereby the crucial part of the A-BER constraint problem is how to find the optimal thresholds that perfectly meets the target BER. The method for computing the optimal SNR thresholds has been proposed in Section 3.2, which entails the analytical solutions for the average spectral efficiency and BER as we derived above.

Take OSTBC for example, the average spectral efficiency and BER can be substituted into (3.8), then we take first order partial derivatives of it with respect to T_k and τ, respectively. The obtained optimal SNR thresholds are plotted in Figure 4.8. Unlike the I-BER constraint case that there is only one set of thresholds for the entire SNR region, every SNR point in this case has a specific set of thresholds. The optimal SNR thresholds decrease in the same pattern as γ_0 increases and a substantial decline is observed when γ_0 exceeds 20dB. This is because as long as the limit of modulation order is achieved at high SNRs, 64-QAM in this case, the extra SNR will contribute to lower the BER. In order to counteract such effect, SNR thresholds must be tuned down to maintain the BER at the same level. However, searching for the optimal SNR thresholds might fail at high SNRs, e.g., $\gamma_0 = 24, 25$dB. This is due to that the approximation given in (3.13) is only accurate in a certain range, $10^{-2} \sim 10^{-5}$. When the approximation is not accurate any more, the optimal solutions are not available. To tackle this situation, we re-use the optimal SNR thresholds obtained when $\gamma_0 = 23$dB.

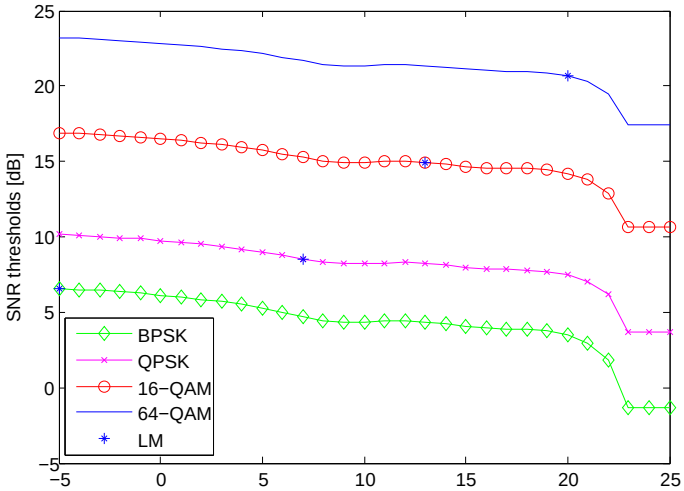

Figure 4.8: *Optimal SNR thresholds for 2×2 OSTBC in spatially correlated Rayleigh fading channels,* $\rho_{tx} = \rho_{rx} = 0.5$.

Provided the optimal SNR thresholds, the resultant average spectral efficiency is shown in Figure 4.9, where the upper bound is the CRSE defined in (3.3). It is observed that the A-BER constraint method, in contrast to the I-BER constraint method, improves spectral efficiency by approximately 1.5dB at medium or high SNRs. However, there still exists a large gap between the average spectral efficiency and the upper bound in low SNR region. This is because the outage probabilities are high at low SNRs when the modulation orders are restricted to discrete integers, but the upper bound assumes continuous-rate modulation orders that offer zero outage. A remedy to enhance the average spectral efficiency at low SNRs is adaptive power allocation, or adaptive channel coding. The improvement by using the adaptive power allocation will be shown in Chapter 5.

4.3 Non-Linear Optimization

It has been shown in the preceding section that the A-BER constraint is able to achieve the maximal average spectral efficiency, but it is computation-demanding to calculate SNR thresholds for every SNR point. A new method will be suggested in this section which can achieve similar performance with limited complexity. More specifically, only one set of SNR thresholds will be determined and they are applicable to the entire SNR region.

Observing that the analytical BERs (4.22,4.23) are functions of the SNR thresholds, it can be formulated as a least squares problem: searching for a set of SNR

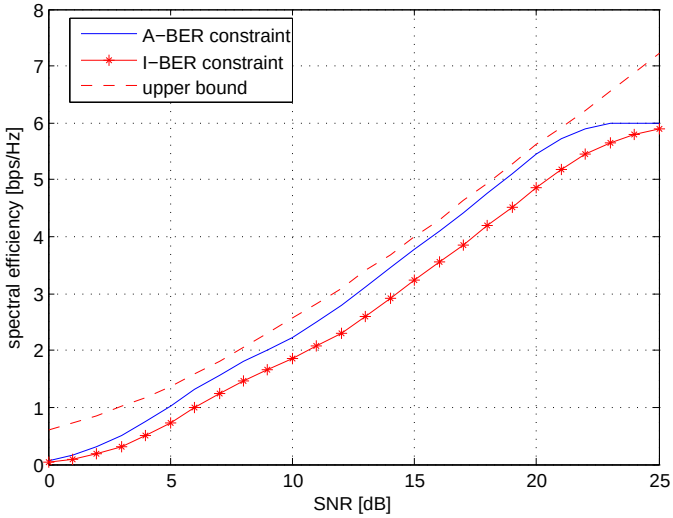

Figure 4.9: *Optimal rate for 2×2 OSTBC in spatially correlated Rayleigh fading channels,* $\rho_{tx} = \rho_{rx} = 0.5$.

thresholds that minimize the sum of the squared differences between the target BER and the analytical BER in the entire SNR region:

$$\mathbf{T}_{\min} = \text{argmin}_{\mathbf{T}} \left\{ \frac{1}{2} \sum_{m=1}^{M} \left| \text{BER}_t - \bar{P}_b(\mathbf{T}, \boldsymbol{\gamma_0}(\mathbf{m})) \right|^2 \right\}, \qquad \mathbf{T} = [T_1, \ldots, T_K],$$

where the factor $1/2$ is introduced for convenience. M is the number of SNR points that are to be examined. Since our interest is the whole SNR region, M is larger than the number of variables, K. This is a typical least squares problem with a nonlinear objective function. An iterative method named Levenberg-Marquardt (LM) algorithm [43] can be used to find the solution. In every iteration, a step size vector $\Delta\mathbf{T}$ is calculated according to

$$\left(\mathbf{J}^T\mathbf{J} + \mu\mathbf{I}\right) \Delta\mathbf{T} = -\mathbf{J}^T\mathbf{f}, \qquad \mu > 0 \tag{4.27}$$

Then the SNR thresholds are updated at every iteration:

$$\mathbf{T}_{l+1} = \mathbf{T}_l + \Delta\mathbf{T} \tag{4.28}$$

Such iteration will stop when $\mathbf{T}_l$ converges. $\mathbf{J}$ is the $M \times K$ Jacobian matrix of the objective function $f = \text{BER}_t - \bar{P}_b$:

$$[\mathbf{J}]_{mk} = \frac{\partial f}{\partial T_k} \Big|_{\mathbf{T}, \gamma_0(m)} = -\frac{\partial \bar{P}_b}{\partial T_k} \Big|_{\mathbf{T}, \gamma_0(m)}, \tag{4.29}$$

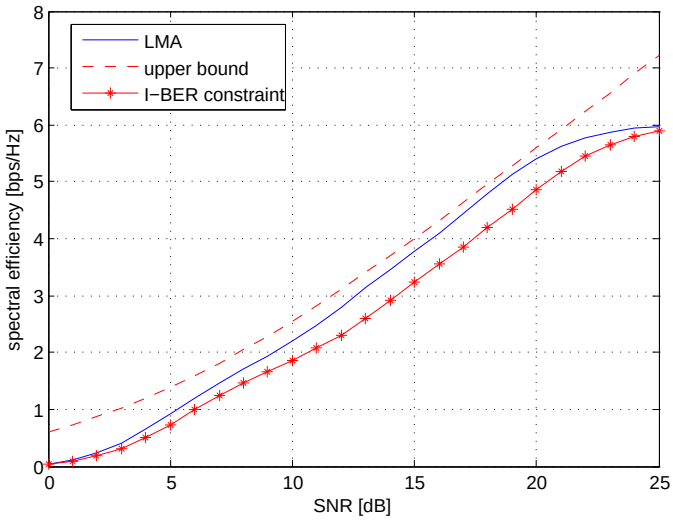

Figure 4.10: *Improvement on spectral efficiency of OSTBC by using the LM algorithm in 2×2 Rayleigh fading channels,* $\rho_{tx} = \rho_{rx} = 0.5$.

$\mathbf{f}$ is an $M \times 1$ vector representing the difference between the target BER and the analytical BER:

$$\mathbf{f} = [\mathrm{BER}_t, \ldots, \mathrm{BER}_t]^T - [\bar{P}_{b,l}(\gamma_0(1)), \ldots, \bar{P}_{b,l}(\gamma_0(M))]^T,$$

where $\bar{P}_{b,l}(\gamma_0(m))$ is the analytical BER at lth iteration when $\gamma_0 = \gamma_0(m)$. μ is the damping factor that ensures $\mathbf{\Delta T}$ is a descent direction. μ has a large value when it is far from the solution and a small value otherwise.

However, it should be noticed that (4.27) can only generate local minima and the optimality of the solution depends on the initial values, $\mathbf{T}_0$. By applying the algorithm to a 2×2 MIMO system in Rayleigh fading channels where $\rho_{tx} = \rho_{rx} = 0.5$, significant improvement on spectral efficiency can be obtained compared to the I-BER constraint case, as shown in Figure 4.10. The newly achieved average spectral efficiency is even comparable to the optimal one as given in Figure 4.9. The resultant BER by using the new SNR thresholds is close to the target BER when SNR is below 20dB, see Figure 4.11. However, when SNR is higher than 20dB, the maximal modulation order is reached and the resulting BER falls steeply below the target. To prevent the BER diverging from the target, much lower SNR thresholds have to be employed, as in the case of A-BER constraint. Therefore, it is impossible to keep the BER to the same level in the whole SNR region.

The SNR thresholds that are employed to obtain the above performance are 6.613dB, 8.579dB, 14.922dB, 20.715dB, which are plotted in Figure 4.8. It is interesting to find that the four points are almost on one straight line.

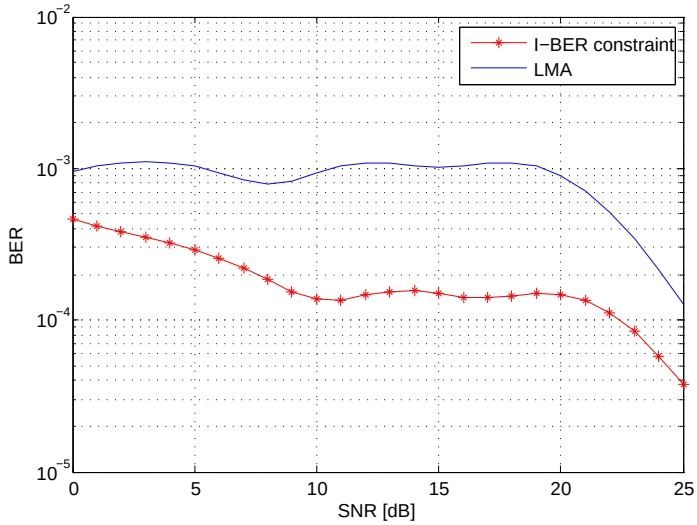

Figure 4.11: *BER of OSTBC by using the SNR thresholds obtained from the LM algorithm in 2×2 Rayleigh fading channels,* $\rho_{tx} = \rho_{rx} = 0.5$.

4.4 Optimal MIMO Scheme

Considering the fact that distinct average spectral efficiencies are achieved by applying different MIMO coding schemes, it is worth identifying the optimal scheme that yields the highest average spectral efficiency among the candidates. If several MIMO coding schemes are simultaneously available at transmitter, choosing the best coding scheme will considerably improve spectral efficiency. Thereafter, besides adaptive modulation, one more degree of freedom can be incorporated into the adaption schemes.

To be able to find the optimal MIMO scheme, we can make use of the closed-form expressions to derive the average spectral efficiencies of every coding scheme. Since the average spectral efficiency is a function of the average SNR and the spatial correlation coefficient, which are statistical information that would not change as time elapses, the selection needs to be done only once, as long as the channel characteristics remain unchanged.

For instance, if there are two MIMO coding schemes available, OSTBC and ZF, in 2×2 i.i.d. Rayleigh fading channels, the average spectral efficiencies are shown in Figure 4.12. By inspection, they have an intersection point at around 18dB. This point can be logged by the transmitter so that it just needs to compare the current operating SNR point to this point to decide which scheme to use, rather than calculating the average spectral efficiency each time when a decision is to

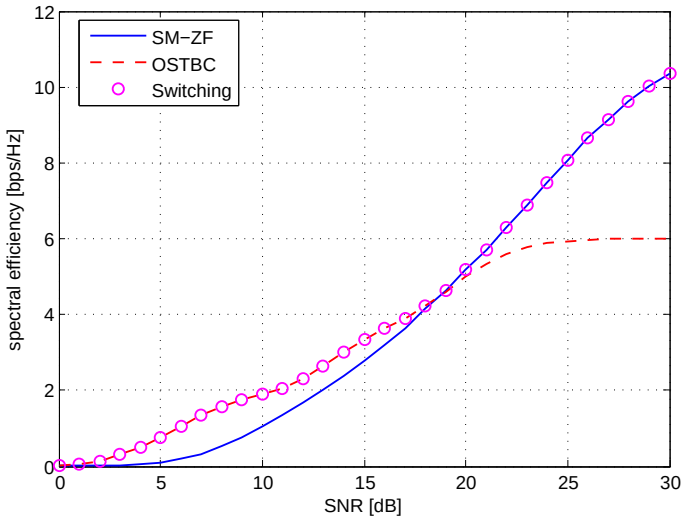

Figure 4.12: *Average spectral efficiencies of ZF-OSTBC in* 2×2 *i.i.d. Rayleigh fading channels.*

be made. Mathematically, the intersection point can be obtained by solving the following equation for γ_0:

$$\overline{\mathrm{SE}}_{ostbc}(\gamma_0) = \overline{\mathrm{SE}}_{zf}(\gamma_0). \tag{4.30}$$

Unfortunately, this equation is intractable, but numerical results can be easily found by using the Newton-Raphson method [44]:

$$\gamma_{n+1} = \gamma_n - \frac{f(\gamma_n)}{f'(\gamma_n)}, \tag{4.31}$$

where $f(\gamma_n) = \overline{\mathrm{SE}}_{ostbc}(\gamma_n) - \overline{\mathrm{SE}}_{zf}(\gamma_n)$ and n is the index of iteration. The iterations converge fast as there is only one intersection point.

As a matter of fact, the intersection point depends not only on the SNR, channel correlation, but also the target BER. If we lower the target BER in Figure 4.12, the average spectral efficiencies will decrease simultaneously and the intersection point will increase. Figure 4.13 shows the dependence of the intersection point on the target BER. The intersection point decreases as we relax the requirement on the target BER.

The selection of the optimal algorithm depends on the SNR only, not the instantaneous channel gains, thus it can be regarded as static adaptation. On the other hand, if we have the luxury to compute the modulation order for OSTBC and ZF, respectively, in every attempt of transmission, and choose the one with the

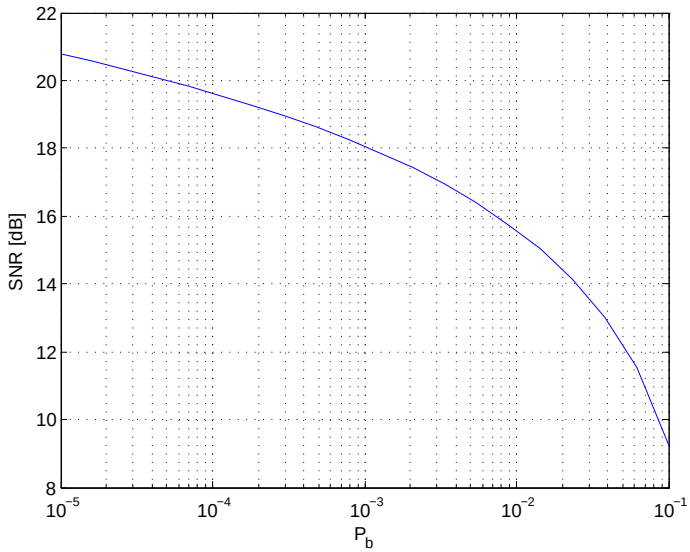

Figure 4.13: *Switching point of ZF-OSTBC in* 2×2 *i.i.d. Rayleigh fading channels.*

higher modulation order, we would definitely obtain a higher spectral efficiency, as shown in Figure 4.14. This can be viewed as dynamic adaptation. The gaps between static adaptation and dynamic adaptation are more noticeable around the intersection points. This is because OSTBC is favored at low SNRs while ZF is more advantageous at high SNRs, thus the dynamic adaptation gain is more pronounced around the intersection points, where the two MIMO schemes have similar performance. Near the intersection points, dynamic adaptation is preferred as it really depends on the instantaneous channel gain to decide which one is better. However, as the number of receive antennas increases, the difference between the two adaptation strategies is vanishing to negligibly small. This is due to that OSTBC and ZF have similar performance around the intersection point in the 2×2 case, the benefit we can get from dynamic adaptation is maximal in light of the uncertainty. As N_r increases, the performance of OSTBC differs distinctly from ZF around the intersection point [45], so the benefit of dynamic adaptation becomes negligible.

4.5 Remarks

So far, we have discussed adaptive modulation and MIMO coding scheme selection in an attempt to improve the average spectral efficiency. More techniques can be used to further improve the average spectral efficiency, e.g., adaptive channel

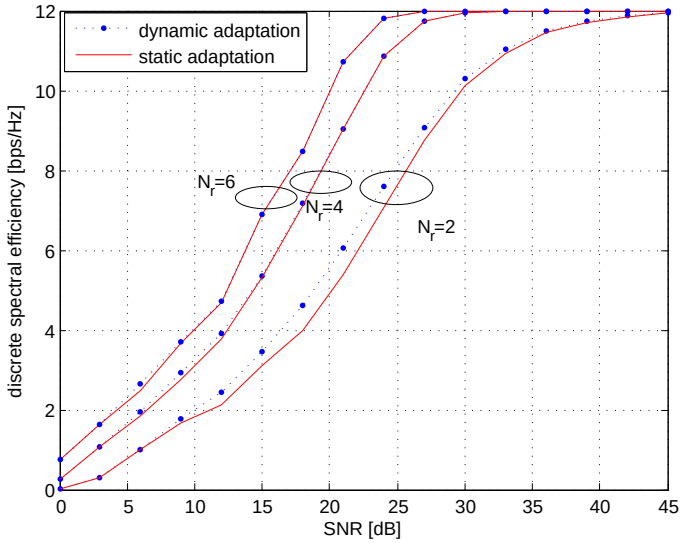

Figure 4.14: *Spectral efficiencies achieved by static adaptation and dynamic adaptation in $N_r \times 2$ i.i.d. Rayleigh fading channels.*

coding, antenna selection, etc.

Channel coding can be used to build a more robust radio link with additional coding gain. An example of adaptive modulation and coding (AMC) using convolutional codes was presented in [46], where the coding rate was adjustable and it was combined with adaptive modulation to obtain better grained fading regions. As a result, a higher average spectral efficiency was achieved in low and moderate SNR regions compared to the uncoded system. Papers [47, 48] demonstrated another type of AMC that superimposed trellis codes on the adaptive modulation.

Considering a transmitter or a receiver with more than required antennas, it is beneficial to select the antennas with better channel quality to boost the performance. For example, if we have more than two transmit antennas for OSTBC, there are two strategies for transmission: 1) use all transmit antennas to achieve the maximal diversity offered by the channel, 2) use only a subset of the transmit antennas that provides the highest effective SNR at the receiver, to avoid wasting power in the weak antenna(s) [49]. The performance of these two strategies is provided in Figure 4.15, where there are 2 receive antennas and 4 transmit antennas for selection. By employing two transmit antennas out of four, antenna selection achieves higher spectral efficiency in most cases. Compared to a normal 2×2 system, antenna selection has approximate 2dB selection gain. More analysis of the performance can be found in [50] and the references therein.

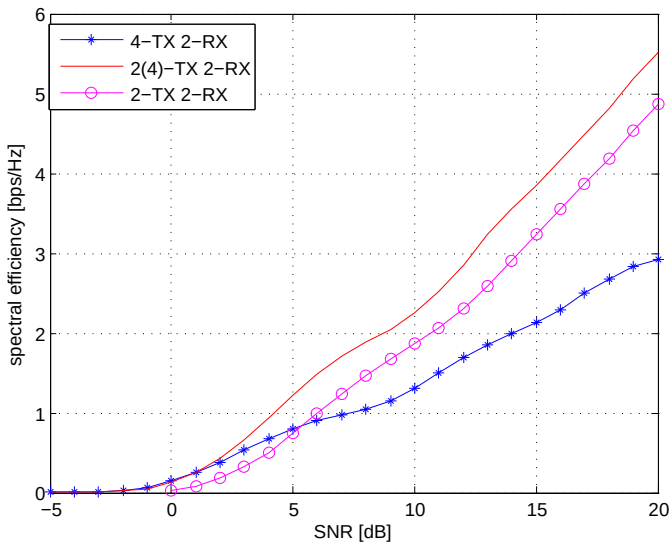

Figure 4.15: *Achievable average spectral efficiency by applying antenna selection in OSTBC systems.*

Chapter 5

Adaptive Power Allocation for MIMO Systems

Adaptive modulation is able to increase average spectral efficiency by adapting modulation order to fading channel. We will, in this chapter, consider adjusting transmit power to further boost the performance. It is well known that the water-filling [65] power allocation can improve the capacity in low SNR region, see Figure 5.1. However, we will show that, under practical circumstances, the power allocation is favorable in high SNR region as well.

A block diagram of adaptive power allocation is shown in Figure 5.2, where the transmit power as well as the modulation order are adjusted based on the CSIT.

This chapter will focus on the realistic improvement that can be achieved by utilizing adaptive power allocation. Other than the famous water-filling algorithm, more practical power allocation strategies will be presented in different scenarios. A major concern of our work is to limit the complexity of the power allocation method for practical purposes.

We will study the power allocation in two MIMO coding schemes, OSTBC and SVD. The power allocation in OSTBC is related to the adaptive modulation scheme with I-BER constraint discussed in Section 4.1, which was originally proposed in [13] for SISO systems. In case of SVD, we will propose a practical power allocation method, subject to peak power constraint and I-BER constraint, which achieves comparable performance to that of the optimal method, namely exhaustive search.

5.1 Variable Transmit Power for OSTBC

Recall the basic adaptation scheme discussed in Section 4.1, we apply fixed SNR thresholds to fulfill the I-BER constraint. However, the resulting BER is always lower than the target. To combat this problem, we relax the requirement on fixed transmit power and allow variable transmit power across time. As the power is adjustable, it is feasible to keep the error probability constant for every channel

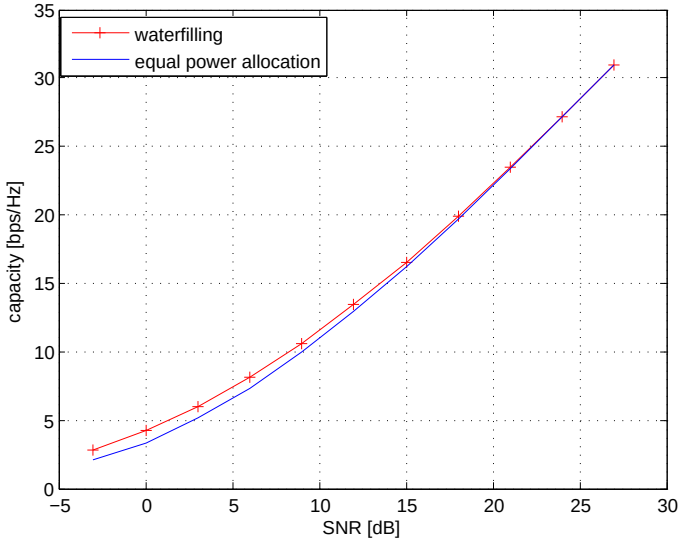

Figure 5.1: *Capacities with and without power allocation in 4×4 MIMO SVD systems.*

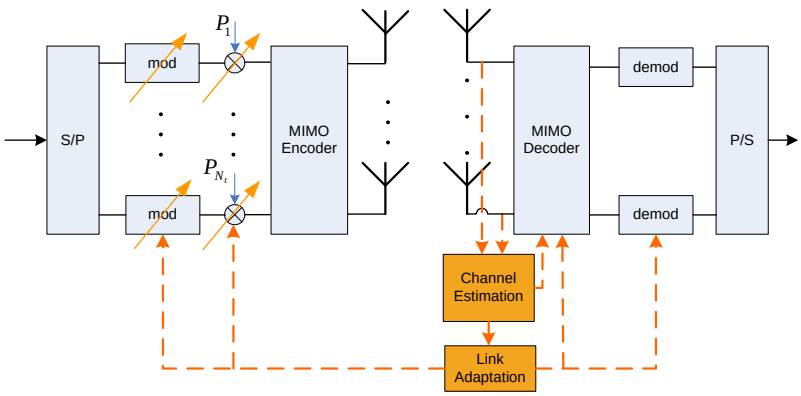

Figure 5.2: *Block diagram of adaptive power allocation and adaptive modulation.*

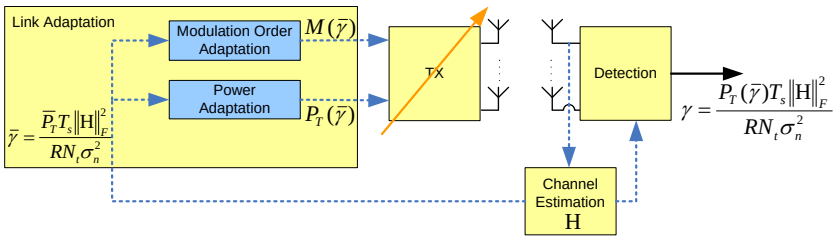

Figure 5.3: *OSTBC systems with adaptive power and modulation.*

realization. As a result, the average BER would be equal to the target after a large number of channel realizations. One way to maintain the instant error probability constant, regardless of the variation of instantaneous channel gain, is to apply channel inversion (CI) power allocation [51]. That is, the transmit power is in the form of $1/\|\mathbf{H}\|_F^2$. In the context of adaptive M-QAM modulation, the power allocation is given as:

$$P_T(\bar{\gamma}) = \frac{\bar{P}_T}{a_k \bar{\gamma}} \ln \frac{c_k}{\mathrm{BER}_t}, \tag{5.1}$$

where a_k and c_k are parameters designed for specific modulation order, as given in Table (3.1), $\bar{\gamma}$ is the effective SNR subject to $\mathbf{H}$ when the transmit power is fixed to the average transmit power, $\bar{P}_T$:

$$\bar{\gamma} = \frac{\bar{P}_T T_s \|\mathbf{H}\|_F^2}{RN_t\sigma_n^2}, \tag{5.2}$$

Other notations are defined the same as in Section 4.1. In this way, the instantaneous SNR at the receiver is:

$$\gamma = \frac{P_T(\bar{\gamma})}{\bar{P}_T}\bar{\gamma} = \frac{1}{a_k} \ln \frac{c_k}{\mathrm{BER}_t}, \tag{5.3}$$

which is a constant at every modulation level. The modulation order is selected by comparing $\bar{\gamma}$, rather than γ, with the SNR thresholds, as shown in Figure 5.3. In other words, the modulation order is determined based on the channel quality, regardless of the instantaneous transmit power. The instantaneous power, on the other hand, is used to counteract the fading of wireless channels.

The optimal SNR thresholds can be found by solving the following problem:

$$\begin{cases} \max\limits_{T_1,\ldots,T_K} & \overline{\mathrm{SE}}(T_1,\ldots,T_K) & \text{(5.4a)} \\ \text{subject to} & \sum\limits_{k=1}^{K} \int_{T_k}^{T_{k+1}} P_T(\bar{\gamma}) p_{\bar{\gamma}}(\bar{\gamma}) d\bar{\gamma} = \bar{P}_T & \text{(5.4b)} \end{cases}$$

where $\overline{\text{SE}}$ denotes the average spectral efficiency calculated by integration, as shown in (3.10). (5.4b) sets the average power constraint. What should be noticed is that the p.d.f. of the effective SNR refers to $p_{\bar{\gamma}}(\bar{\gamma})$ in this context. The optimal solutions of $\{T_1, \ldots, T_K\}$ could be found by taking derivatives of J with respect to T_k, $k = 1 \ldots, K$, where J is the Lagrangian multipliers:

$$J(T_1, \ldots, T_K, \tau) = \overline{\text{SE}} + \tau \left(\sum_{k=1}^{K} \int_{T_k}^{T_{k+1}} P_T(\bar{\gamma}) p_{\bar{\gamma}}(\bar{\gamma}) d\bar{\gamma} - \bar{P}_T \right) \tag{5.5}$$

Through some manipulations, the SNR thresholds are obtained:

$$\begin{cases} T_1 = \dfrac{\tau}{a_1 d_1} \ln \dfrac{\text{BER}_t}{c_1} & \text{(5.6a)} \\ T_k = \dfrac{\tau}{\Delta d_k} \left(\dfrac{1}{a_k} \ln \dfrac{\text{BER}_t}{c_k} - \dfrac{1}{a_{k-1}} \ln \dfrac{\text{BER}_t}{c_{k-1}} \right) & \text{(5.6b)} \end{cases}$$

where $\Delta d_k = d_k - d_{k-1}$, τ is solved numerically from the power constraint:

$$\sum_{k=1}^{K} \int_{T_k}^{T_{k+1}} P_T(\bar{\gamma}) p_{\bar{\gamma}}(\bar{\gamma}) d\bar{\gamma} = \bar{P}_T \tag{5.7}$$

Since the p.d.f. of $\bar{\gamma}$ is needed to solve the problem, we can divide the solution into two cases as we did in Section 4.1, one for non repeated-roots and the other is repeated-roots. Inserting the p.d.f. into (5.7), we may obtain the numerical result for τ and eventually the optimal SNR thresholds. An example of optimal SNR thresholds are shown in Figure 5.4, as a function of γ_0.

It is worth noticing that there are three modulation orders provided in the system, QPSK, 16-QAM, and 64-QAM. The reason that we exclude 8-QAM and 32-QAM from the modulation order list is that the contributions of 8-QAM and 32-QAM in adaptive modulation systems is unnoticeable, as shown in Figure 5.5. Furthermore, BPSK is not included, either. This is due to that BPSK and QPSK can not coexist in this case. Because every SNR threshold must fulfill (5.6a) and (5.6b), to be able to arrive at the desired average transmit power. However, BPSK and QPSK can not meet this condition, provided the parameter values as shown in Table 3.1. Therefore, we choose QPSK over BPSK since QPSK can achieve higher average spectral efficiency. As shown in Figure 5.5, QPSK outperforms BPSK in both cases: with and without 8-QAM, 32-QAM. Therefore, we restrict the available modulation orders to $\{0, 4, 16, 64\}$ in the following discussions. The elimination of the three modulation orders from the list significantly simplifies the adaptation scheme and less feedback information is required.

Figure 5.6 and 5.7 compare the average spectral efficiency with and without power allocation in various OSTBC systems, where an orthogonal code design with $R = 1/2$ is utilized in 4×4 systems [5]. Significant improvement is observed by applying power allocation. In 2×2 systems, an approximate 3dB gain is achieved at medium and high SNRs, while even higher gains are achieved at low SNRs. Besides, at least 2dB gain is achieved in 4×4 systems.

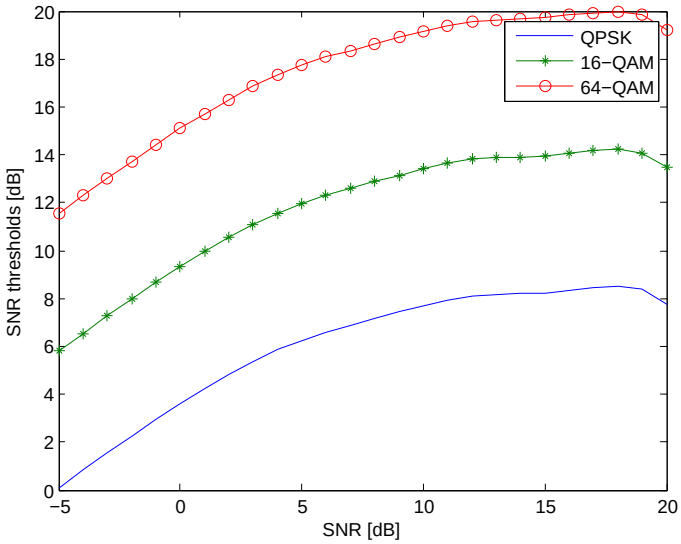

Figure 5.4: *Optimal SNR thresholds for* 2×2 *OSTBC in spatially correlated Rayleigh fading channels,* $\rho_{tx} = 0.4, \rho_{rx} = 0.3$.

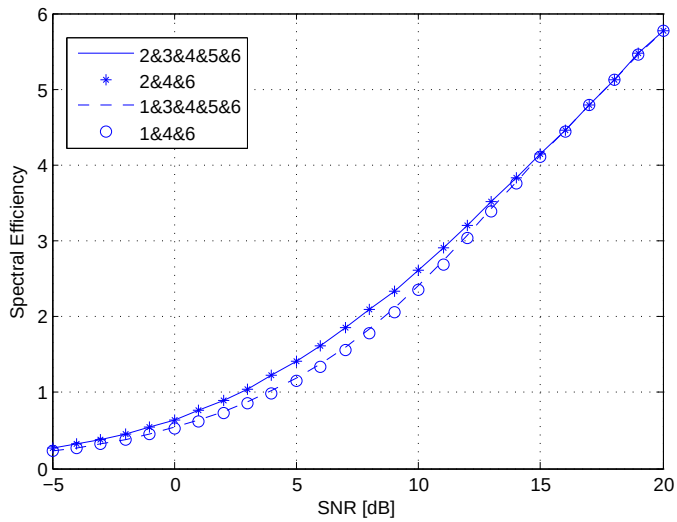

Figure 5.5: *Spectral efficiencies of* 2×2 *OSTBC in spatially correlated Rayleigh fading channels,* $\rho_{tx} = 0.4, \rho_{rx} = 0.3$.

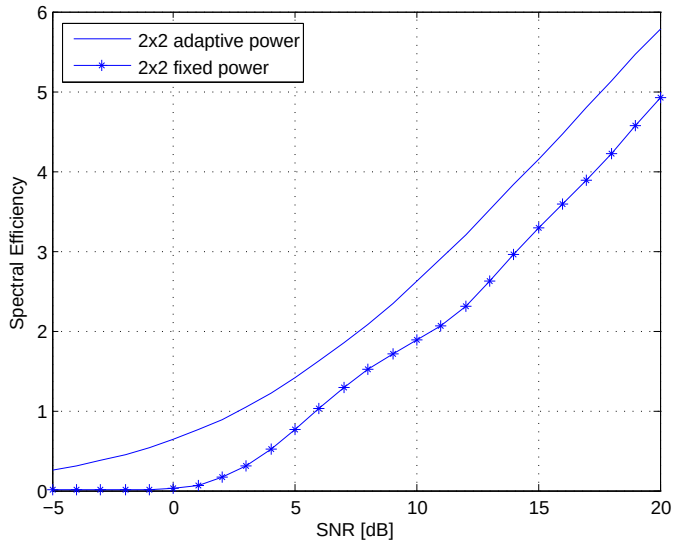

Figure 5.6: *Comparison of average spectral efficiencies with and without power allocation in 2×2 OSTBC,* $\rho_{tx} = 0.4, \rho_{rx} = 0.3$.

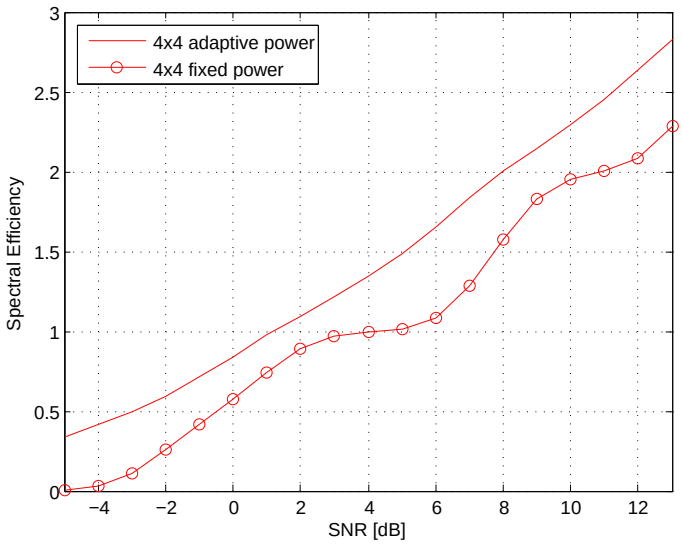

Figure 5.7: *Comparison of average spectral efficiencies with and without power allocation in 4×4 OSTBC,* $\rho_{tx} = 0.4, \rho_{rx} = 0.3$.

Further Discussions

Although the power allocation described above can considerably improve the average spectral efficiency, it is not yet the optimal scheme. The instant error probability is strictly forced to the target level, as long as the channel quality is good enough. This is, in a sense, truncated channel inversion as suggested in [51]. If we can relax the stringent requirement on the instant error probability and allow A-BER constraint, better performance should be obtained. The problem can formulated as follows:

$$\begin{cases} \max\limits_{T_1,\ldots,T_K,P_T(\bar{\gamma})} & \overline{\mathrm{SE}}(T_1,\ldots,T_K,P_T(\bar{\gamma})) & \text{(5.8a)} \\ \text{subject to} & \int_0^{+\infty} P_T(\bar{\gamma})p_{\bar{\gamma}}(\bar{\gamma})d\bar{\gamma} = \bar{P}_T & \text{(5.8b)} \\ & \sum\limits_{k=1}^{K}\int_{T_k\bar{P}_T/P_T(\bar{\gamma})}^{T_{k+1}\bar{P}_T/P_T(\bar{\gamma})} P_b(\gamma,M_k)p_{\bar{\gamma}}(\bar{\gamma})d\bar{\gamma} = \mathrm{BER}_t & \text{(5.8c)} \end{cases}$$

This is similar to what has been done in [13] for the SISO case, where the optimal solution is not available and only a suboptimal solution could be found. Moreover, it should be noted that the performance based on the suboptimal solution is worse than that achieved by maintaining the instant error probability [13]. The results are summarize in Table 5.1.

constraints	average BER	instantaneous BER
average power	(5.8a-5.8c)	(5.4a-5.4b)

Table 5.1: *Optimal power control schemes for discrete-rate QAM signals in OSTBC systems.*

5.2 Variable Transmit Power for SVD

A major difference between SVD and OSTBC is that there are several parallel sub-channels established by SVD while OSTBC has only one sub-channel. In that sense, OSTBC resembles SISO and the adaptation in OSTBC can be treated in the same way as in SISO systems. When it comes to SVD or other coding schemes that are featured by multiple sub-channels, the problem becomes more complicated as the adaptation can be conducted both across time and space. To deal with the problem, [16] made use of unordered eigenvalue distribution to convert the spatial and temporal adaptation to a temporal adaptation only, i.e., similar to the adaptation in SISO scenario. In this part, we will restrict the adaptation within spatial domain and impose fixed transmit power constraint over time. It can be viewed as peak power constraint problem since the sum of the transmit power on

every antenna should be bounded by the total power. We can extend Table 5.1 by adding the peak power constraint:

Constraint	average BER	instantaneous BER
average power	Lagrangian [13]	Lagrangian [16]
peak power	?	exhaustive search [21]

Table 5.2: *Optimal power control schemes for discrete-rate QAM signals in SVD systems.*

By imposing the average constraints on BER and power, the power allocation and SNR thresholds were derived by Lagrangian multipliers in [13][1]. Substituting the A-BER constraint with the I-BER constraint makes the problem more tractable and the optimal solutions were found in [16]. However, as far as we know, the optimal solution subject to the A-BER constraint and peak power constraint is not yet available. In this section, we concentrate on schemes subject to the I-BER constraint and the peak power constraint, which is of the lowest complexity out of the four categories. Although the optimal solution is found to be the exhaustive search [21], other power control schemes can be employed to reduce the computational complexity.

The mechanism of adaptive modulation and power allocation is shown in Figure 5.8, where the modulation order is decided based on the effective SNR γ_i, eventually the channel quality as well as the instantaneous transmit power. In contrast to the case of OSTBC, the instantaneous transmit power P_i herein is used to boost the modulation order.

Practical Power Allocation Schemes

In light of the prohibitive complexity exhibited by the exhaustive search, several simpler power control schemes are proposed, e.g., water-filling [36], uniform power allocation with transmit antenna selection (TAS), and greedy power allocation [52]. Before presenting the greedy power allocation method, we briefly outline the other two power control schemes.

Water-Filling

Since water-filling is the optimal power allocation algorithm for channel capacity as well as CRSE, we use the power scheme suggested for CRSE case [21]:

$$P_i = \left(\xi - \frac{\sigma_n^2}{K_o \lambda_i}\right)_+, i = 1, 2, \cdots, N_s, \tag{5.9}$$

[1]The optimal power allocation is obtained, but the optimal solution for SNR thresholds is not available. Instead, a suboptimal solution for thresholds are obtained and this results in worse performance than the I-BER constraint.

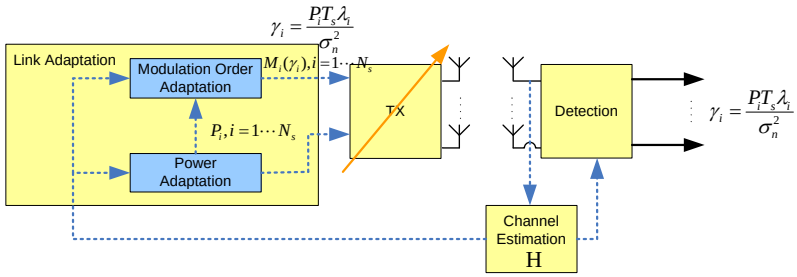

Figure 5.8: *SVD systems with adaptive power and modulation.*

where ξ is chosen to satisfy the peak power constraint, K_o is the SNR gap between the capacity and the achievable rate by using continuous-rate QAM modulation. The bit-loading is carried out by comparing the effective SNR, $P_i T_s \lambda_i / \sigma_n^2$, with the SNR thresholds given by (4.1). Noticeably, it is unavoidable to waste some amount of power by using this approach. For instance, water-filling may allocate a certain amount of power to a weak sub-channel, but it does not guarantee to reach the lowest SNR threshold.

Uniform Power Allocation with TAS

To avoid any abuse of the transmit power, uniform power allocation can be applied to assign power only to the sub-channels that can support at least the lowest modulation order. The selection of the sub-channels is based on the criterion that the effective SNR of the weakest sub-channel must be larger than the smallest SNR threshold T_1. The process is described in Table 5.3.

Greedy Power Allocation

The idea of greedy power allocation is to assign as much power as possible onto the strongest sub-channel to achieve the possibly maximal modulation order. Provided the fact that:

$$\lambda_1 > \lambda_2 > \ldots > \lambda_{N_{\min}},$$

where $N_{\min} = \min\{N_t, N_r\}$, the power allocation can be done in an order from the strongest singular value channel ($i = 1$) to the weakest one ($i = N_{\min}$). More detailed process is illustrated in Table 5.4.

The complexity of the greedy power allocation is of the same order as that of the water-filling and the uniform power allocation with TAS, i.e., $O(N_{\min})$. On the other hand, the exhaustive search is of complexity $O(N_{\min}^{N_{\min}})$.

Uniform power allocation with TAS	
1.	Initialize the number of selected sub-channels: $N_s = N_{\min}$
2.	Calculate the effective SNR on the sub-channel with smallest singular value: $$\gamma_{N_s} = \frac{P_T T_s \lambda_{N_s}}{N_s \sigma_n^2},$$ if $\gamma_{N_s} > T_1$, go to step 4, otherwise go to step 3
3.	Remove the weakest sub-channel: $N_s = N_s - 1$. If $N_s > 0$, go to step 2, otherwise go to step 4
4.	The end.

Table 5.3: *Uniform power allocation with TAS.*

Greedy power allocation	
1.	Let $\Delta P = P_T$ and $i = 1$
2.	Find the maximum rate r_i that the sub-channel i can support with ΔP
3.	Calculate the desired power to achieve the rate r_i: P_i Re-calculate the residual power: $\Delta P = \Delta P - P_i$
4.	Go to the next strongest sub-channel: $i = i + 1$, if $i \leq N_{\min}$ and $\Delta P > 0$, go to step 2; otherwise, go to step 5
5.	The end.

Table 5.4: *Greedy power allocation.*

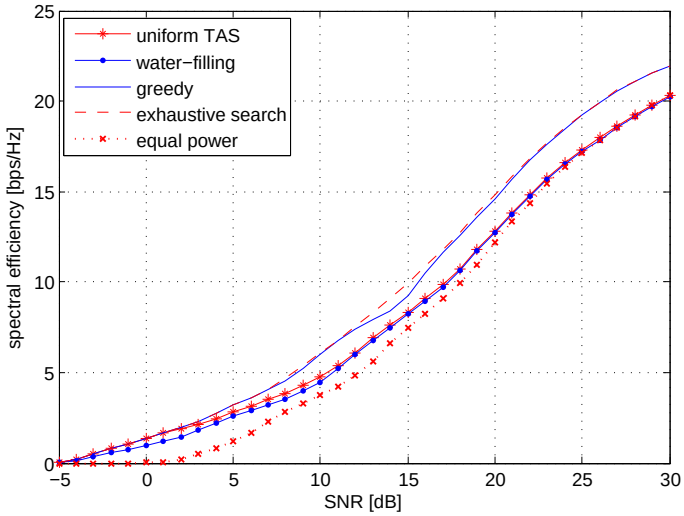

Figure 5.9: *Spectral efficiencies of power control schemes in* 4×4 *i.i.d Rayleigh fading channels.*

A Comparison of Power Control Schemes

We have reviewed three power allocation policies, water-filling, uniform power allocation with TAS, and greedy power allocation. The performance are compared against that of the exhaustive search in two different channel environment: i.i.d. Rayleigh fading channels and spatially correlated Rayleigh fading channels.

In 4×4 i.i.d. Rayleigh fading channels, the spectral efficiencies achieved by utilizing different power control schemes are shown in Figure 5.9. It is observed that the average spectral efficiency achieved by using greedy power allocation is almost as good as the performance of the exhaustive search. It outperforms the water-filling method by about 3dB at high SNRs. The uniform power allocation with TAS is able to reach the same performance as the greedy allocation in low SNR region, where only one sub-channel is used. As SNR increases, the performance of the uniform power allocation with TAS resembles that of the water-filling. This is because they are asymptotic to equal power allocation, which is favored at high SNRs. The optimal power allocation scheme is 3dB or so better compared to the equal power allocation in all cases, not just in low SNR region.

In case there are not sufficient scatters around the transmitter and the receiver, correlation exists between any pair of the transmit and the receive antennas. Under this condition, the average spectral efficiencies of different power control schemes are shown in Figure 5.10. We notice that the discrepancy between the greedy allocation and the exhaustive search becomes negligible. The difference between

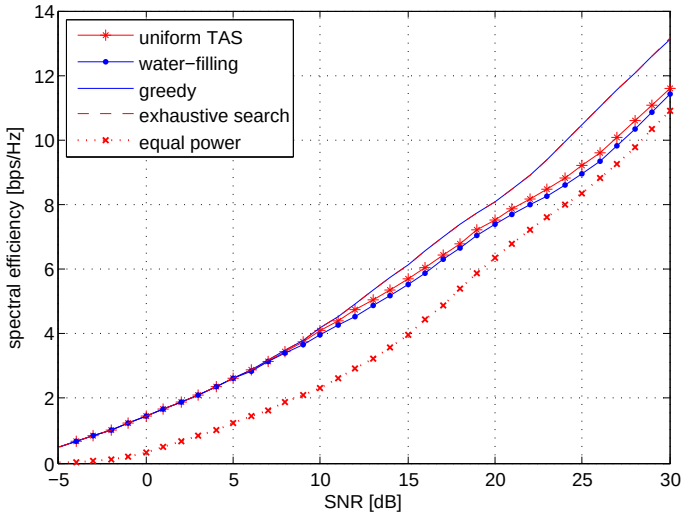

Figure 5.10: *Spectral efficiencies of power control schemes in* 4×4 *spatially correlated Rayleigh fading channels, with* $\rho_{tx} = \rho_{rx} = 0.9$.

the water-filling and the greedy allocation is vanishing in low SNR region, but is more pronounced when SNR is high. The uniform power allocation with TAS is essentially equivalent to the beamforming in low SNR region. As expected, it achieves the maximal spectral efficiency in both scenarios in low SNR region. The gap between the greedy power allocation and the equal power allocation increases to 4-5dB in this scenario.

From the above two figures, we can conclude that

1. greedy power allocation is superior to the water-filling method in practice.

2. Greedy power allocation can achieve comparable performance to the optimal solution with substantially decreased complexity.

3. The performance discrepancy between the greedy algorithm and the optimal exhaustive search method is vanishing as spatial correlation increases.

4. The uniform power allocation with TAS achieves slightly better performance than the water-filling, but is inferior to the greedy algorithm.

5. Good power allocation schemes. e.g., the exhaustive search and the greedy algorithm, are always better than equal power allocation scheme, especially when spatially correlated channels are concerned.

Further Discussion

Water-filling is claimed to be capacity-optimal under the assumption of Gaussian coding and infinite coding length. In practice, however, M-PSK and M-QAM modulation are used instead of Gaussian signals and the water-filling turns out not to be optimal any more, as shown in previous discussions. Although the optimal performance is obtained by adopting the exhaustive search, this application is hindered in practice due to its intensive complexity. Theoretical optimal solutions catering to uncoded M-QAM and M-PSK modulation is expected. By taking into account the exact modulation schemes, a mercury/water-filling power control strategy is suggested in [53], where the gap between Gaussian signal and the practical modulation scheme on each sub-channel is filled by "mercury" first and "water (power)" is poured on top of the mercury. In case of Gaussian signals, the gap is zero and this method boils down to water-filling.

Chapter 6

Adaptation Techniques with Imperfect Channel Estimation

We have reviewed the adaptation techniques in Chapter 3, 4, and 5, when perfect CSI is assumed at both the receiver and the transmitter. In this chapter, we will extend our discussions to imperfect CSI situations. Specifically, we will concentrate on the impact of channel estimation errors on the overall performance of adaptive modulation and adaptive power allocation in OSTBC systems.

Normally, imperfect CSI is incurred at two places, channel estimation and feedback. Noisy channel estimation can cause random interference in the detection which can not be eliminated. Feedback introduces delay as well as errors when passing information from the receiver to the transmitter. Usually, the feedback delay is of more interest as the errors can be avoided by using low modulation order and powerful coding techniques. The feedback delay influences the accuracy of the modulation order, as discussed in [10]. An effective approach to combat the feedback delay is to predict the channel values, as proposed in [69].

6.1 System Model

Let $\hat{\mathbf{H}}$ denote the estimated channel, it can be modeled as [74]:

$$\hat{\mathbf{H}} = \mathbf{H} + \mathbf{\Xi}, \tag{6.1}$$

where Ξ is the estimation noise with independent complex Gaussian entries, $[\Xi]_{ij} \sim \mathcal{CN}(0, \sigma_\epsilon^2)$. $\mathbf{H}$ is the actual channel matrix as defined in (2.1). From (6.1), the original channel can be rewritten as:

$$\mathbf{H} = \eta\hat{\mathbf{H}} + \sqrt{1-\eta}\mathbf{W}, \tag{6.2}$$

where $\eta = \dfrac{1}{1+\sigma_\epsilon^2}$. $\eta = 1$ when channel estimation is perfect. $\mathbf{W}$ is i.i.d. Gaussian white noise, $[\mathbf{W}]_{ij} \sim \mathcal{CN}(0,1)$. Since $\mathbf{H}$ is not available at the receiver, $\hat{\mathbf{H}}$ is

employed in the MRC to recover the transmitted signal, the decision statistic can be written as:

$$\hat{x}_i = \frac{\eta\|\hat{\mathbf{H}}\|_F^2}{R} x_i + \underbrace{I(\mathbf{x}) + \hat{z}}_{\hat{n}} \tag{6.3}$$

where $I(x)$ is the interference due to channel estimation errors. Approximately, it can be treated as uncorrelated white Gaussian noise (Chapter 6, [38]) with variance $\sigma_I^2 = (1-\eta)E_s\|\hat{\mathbf{H}}\|_F^2/R$. $\hat{z}$ is the white noise after matched filter, $\sigma_{\hat{z}}^2 = \|\hat{\mathbf{H}}\|_F^2\sigma_n^2/R$. The resulting SNR is given by

$$\hat{\gamma} = \frac{\eta^2\|\hat{\mathbf{H}}\|^4 E_s/R^2 N_t}{\sigma_I^2 + \sigma_{\hat{z}}^2} = \frac{u\gamma_0\|\hat{\mathbf{H}}\|_F^2}{RN_t}, \tag{6.4}$$

Compared to the effective SNR in perfect CSI scenario (2.25), (6.4) has a factor u that represents the degradation due to the channel estimation noise:

$$u = \frac{\eta^2}{(1-\eta)\gamma_0 + 1} \tag{6.5}$$

As can be seen in (6.4), the effect of estimation noise is reflected in the effective SNR by factor u, which leads to damped SNRs as shown in Figure 6.1, where the output SNR

$$\gamma_{\text{output}} = u\gamma_0 = \frac{\gamma_0}{\sigma_\epsilon^2(1+\sigma_\epsilon^2)\gamma_0 + 1} \tag{6.6}$$

As $\gamma_0 \to \infty$, $\gamma_{\text{output}} \to \frac{\eta}{\sigma_\epsilon^2}$. Therefore, in presence of estimation noise, the damped SNRs start to converge to a constant as the input SNRs increase.

6.2 Adaptive Modulation with Imperfect CSI

The adaptive modulation schemes suggested in Section 3.2 is still applicable to systems with imperfect CSI. To tolerate the interferences caused by the estimation errors, the newly estimated effective SNR $\hat{\gamma}$, instead of γ, is employed in choosing the fading region and the associated modulation order. To obtain the p.d.f. of the effective SNR, we revise the MGF as:

$$M_{\hat{\gamma}}(s) = \prod_{i=1}^{N_r}\prod_{j=1}^{N_t} \frac{1}{1-\hat{\alpha}_{i,j}s}, \tag{6.7}$$

where $\hat{\alpha}_{i,j} = u\left(\alpha_{i,j} + \frac{\gamma_0\sigma_\epsilon^2}{RN_t}\right)$ and $\alpha_{i,j}$ is defined as in (4.13). If the channel estimation is perfect, $\hat{\alpha}_{ij}$ reduces to α_{ij} and the MGF in (6.7) would be equivalent to the MGF given in (4.14). If every $\hat{\alpha}_{i,j}$ has multiplicity 1, namely that is no repeated roots in the MGF, the p.d.f. of $\hat{\gamma}$ can be revised as follows:

$$p_{\hat{\gamma}}(\hat{\gamma}) = \sum_{i=1}^{N_r}\sum_{j=1}^{N_t} \frac{\hat{\varphi}_{i,j}}{\hat{\alpha}_{ij}} e^{-\frac{\hat{\gamma}}{\hat{\alpha}_{ij}}}, \tag{6.8}$$

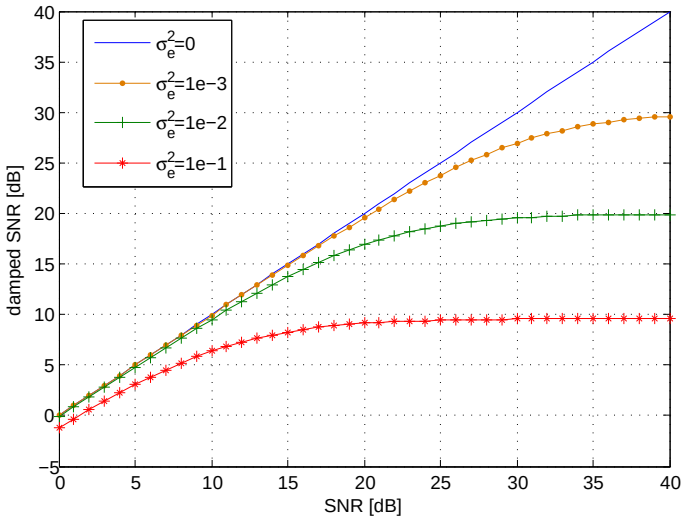

Figure 6.1: *Impact of channel estimation noise: damped SNR = u·SNR.*

where $\hat{\varphi}_{i,j} = (1-\hat{\alpha}_{ij})M_{\hat{\gamma}}(s)\big|_{s=1/\hat{\alpha}_{ij}}$ If there exists repeated $\hat{\alpha}_{i,j}$, let $\hat{\alpha}_m$ denote the distinct values of $\hat{\alpha}_{i,j}$ and $N_s(m)$ represent the multiplicity of each $\hat{\alpha}_m$, the p.d.f. is provided as follows:

$$p_{\hat{\gamma}}(\hat{\gamma}) = \sum_{m=1}^{N_d} \sum_{l=1}^{N_s(m)} \frac{\hat{\varphi}_{m,l}\hat{\gamma}^{l-1}}{\Gamma(l)\hat{\alpha}_m^l} e^{-\frac{\hat{\gamma}}{\hat{\alpha}_m}}, \tag{6.9}$$

where

$$\hat{\varphi}_{m,l} = \frac{(-1/\hat{\alpha}_m)^{N_s(m)-l}}{(N_s(m)-l)!} \frac{d^{N_s(m)-l}}{ds^{N_s(m)-l}} \Big[(1-\hat{\alpha}_m s)^{N_s(m)} M_{\hat{\gamma}}(s)\Big]\Big|_{s=1/\hat{\alpha}_m} \tag{6.10}$$

By replacing $p_\gamma(\gamma)$ with $p_{\hat{\gamma}}(\hat{\gamma})$ in (3.10), the closed-form expressions of performance subject to the I-BER constraint can be obtained:

$$\widehat{\overline{\mathrm{SE}}}_{\mathrm{I}}(\gamma_0, \rho_{tx}, \rho_{rx}, \sigma_\epsilon^2) = R \sum_{k=1}^{K} \sum_{i=1}^{N_r} \sum_{j=1}^{N_t} \hat{\varphi}_{i,j} \Delta d_k e^{-\frac{T_k}{\hat{\alpha}_{i,j}}} \tag{6.11}$$

for non repeated roots case and

$$\widehat{\overline{\mathrm{SE}}}_{\mathrm{II}}(\gamma_0, \rho_{tx}, \rho_{rx}, \sigma_\epsilon^2) = R \sum_{k=1}^{K} \sum_{m=1}^{N_d} \sum_{l=1}^{N_s(m)} \frac{\hat{\varphi}_{m,l}}{\Gamma(l)} \Delta d_k \Gamma_u\big(l, \frac{T_k}{\hat{\alpha}_m}\big) \tag{6.12}$$

for repeated roots case. It is important to notice that (6.11) and (6.12) are more generalized expressions that can be used to evaluate the average spectral efficiencies with or without channel estimation noise. Based on the SNR thresholds suggested for the I-BER constraint, we can use the LM algorithm to find a particular set of SNR thresholds that approach the target BER and hence improve the average spectral efficiency. On the other hand, if we apply the A-BER constraint to the adaptive systems, the optimal SNR thresholds can be computed as suggested in (3.9a-3.9b). The resulting average spectral efficiencies by applying these methods are shown in Figure 6.2, in which the upper bound is the continuous-rate spectral efficiency of QAM modulation with imperfect channel estimation:

$$\widehat{\overline{\mathrm{SE}}}_{ub} = \mathbf{E}_{\hat{\mathbf{H}}}\left\{R\log\left(1+K_o u\gamma\right)\right\} = \overline{R\log\left(1+\frac{K_o\eta^2\gamma_0\|\hat{\mathbf{H}}\|_F^2}{RN_t(1+(1-\eta)\gamma_0)}\right)}, \tag{6.13}$$

As γ_0 keeps increasing,

$$\widehat{\overline{\mathrm{SE}}}_{ub} \to \overline{R\log\left(1+\frac{K_o\eta^2\|\hat{\mathbf{H}}\|_F^2}{RN_t(1-\eta)}\right)} \tag{6.14}$$

In other words, due to the interference caused by the estimation errors, increasing SNR does not necessarily boost spectral efficiency any more, as shown in Figure 6.2.

6.3 Adaptive Power Allocation with Imperfect CSI

This section could be regarded as an extension of the power allocation with perfect channel estimation in Section 5.1. To be able to revise the SNR thresholds, we need the p.d.f. of $\hat{\bar{\gamma}}$, which is defined as:

$$\hat{\bar{\gamma}} = u\bar{\gamma} = \frac{u\gamma_0\|\hat{\mathbf{H}}\|_F^2}{RN_t}, \tag{6.15}$$

where u is the damping factor as defined in (6.5). Given the distribution of $\|\hat{\mathbf{H}}\|_F^2$, the p.d.f. of $\hat{\bar{\gamma}}$ can be found and it is used to solve for the constant τ that guarantees the average power constraint (5.7). By plugging τ into (5.6a) and (5.6b), we arrive at the SNR thresholds for imperfect channel estimation.

In presence of channel estimation noise, the average spectral efficiency is deteriorated due to the unremovable interference. Moreover, the interference increases in proportion to SNR, that is, the degradation of spectral efficiency is more serious in high SNR region, as shown in Figure 6.3. The average spectral efficiencies when $\sigma_\epsilon^2 = 10^{-3}, 10^{-2}, 10^{-1}$ are compared to the one with perfect channel estimation. The degradation becomes substantial as the estimation noise power exceeds 10^{-2}. The corresponding BERs are shown in Figure 6.4, where the actual BERs diverge

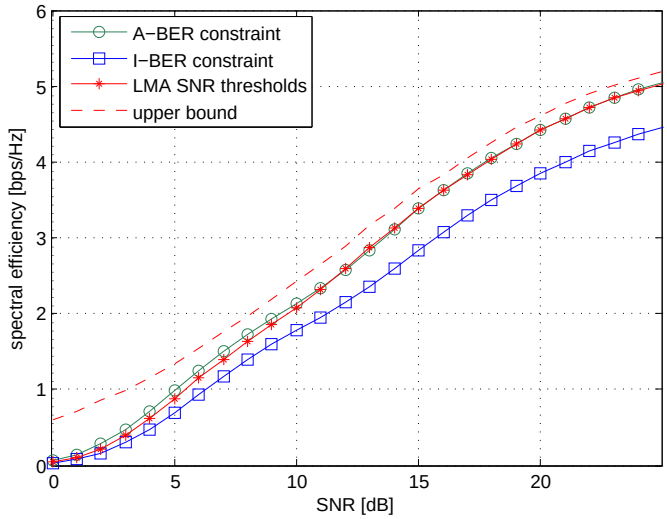

Figure 6.2: *Average spectral efficiency with imperfect channel estimation, in 2×2 spatially correlated Rayleigh fading channels,* $\rho_{tx} = \rho_{rx} = 0.5$, $\sigma_\epsilon^2 = 0.01$.

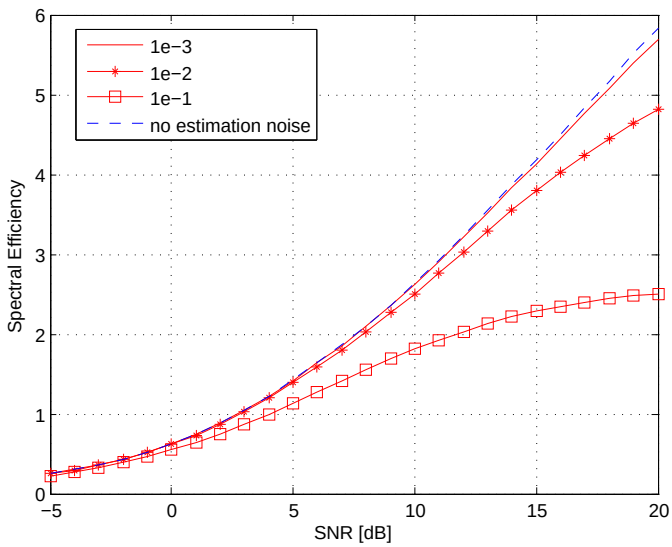

Figure 6.3: *Average spectral efficiency of OSTBC with imperfect CSI in* 2×2 *i.i.d. Rayleigh fading channels.*

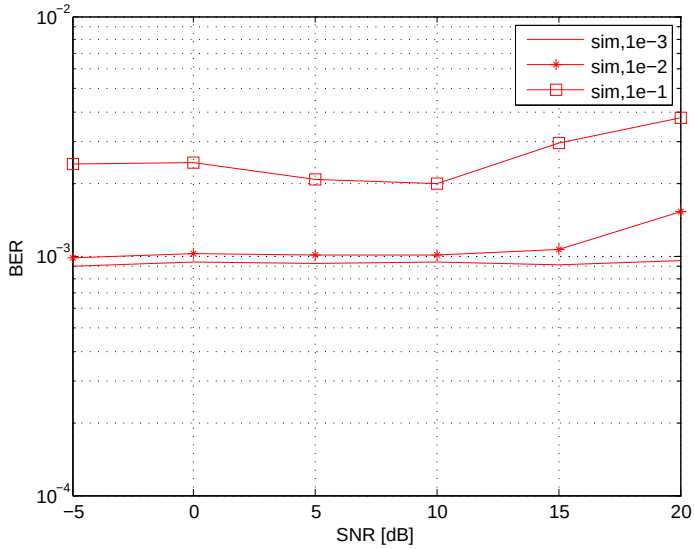

Figure 6.4: *BER of OSTBC with imperfect CSI in* 2×2 *i.i.d. Rayleigh fading channels.*

from the predefined target, 10^{-3}. When the estimation noise $\sigma_\epsilon^2 > 10^{-2}$, the resultant BER is higher than the target and the discrepancy becomes more prominent as SNR increases. This can be explained by the ratio of the interference and the white noise within $\hat{n}$ in (6.3). For low ratios, the white Gaussian noise is the dominating part and it is acceptable to treat $\hat{n}$ as white Gaussian noise. The resulting performance of BER is approximately equal to the target. If, on the other hand, the ratio is high and the interference becomes the dominating factor, the approximation to white Gaussian noise is questionable. As a consequence, the actual BERs diverge from the target level.

6.4 Remarks

In this chapter we extend the discussion of adaptive modulation and adaptive power allocation by considering the effect of imperfect channel estimation. To deal with the estimation errors, a modified effective SNR is employed in selecting the modulation order and it leads to decreased average spectral efficiencies. By this means, the interference caused by imperfect estimation is treated as white noise. However, the approximation of the interference as noise is only valid when the ratio between the interference power and the noise power is low, otherwise it would result in divergence of the actual BER from the predefined target.

Chapter 7

Link Layer Simulator (LiLaS)

This chapter will present a generic Link Layer Simulator (LiLaS)[1] for multiple antenna systems in the MATLAB and OCTAVE environments, for both Windows and Unix/Linux operating systems. The development of LiLaS is originated from the idea of Software Defined Radio (SDR). As a promising solution for the fast developing radio communications, SDR has been suggested as a generic platform for various radio architectures. The idea of SDR is to put the AD/DA converters as close as possible to the antennas and operate as much as possible in the digital domain by software. In this way, the transceivers are reconfigurable to support different protocols. To meet this objective, the simulator is functionally divided into modules, sub-modules and models with a common interface for the convenience of modification and reconfiguration.

Currently, it accommodates a variety of modulation and coding schemes, including single-carrier MIMO, OFDM, MIMO-OFDM, OFDM/Offset QAM, and DS-CDMA.

7.1 Simulator Architecture

The main function of the simulator is called 'LiLaS.m', the execution of which is divided into three phases: setup (initialization of all functions and parameters), run (data transmission), and wrapup (result calculations and presentations).

Inside every phase, the modules are called in a specified order. There are five main modules: *SOURCE*, *TX*, *CH*, *RX* and *SINK*, as shown in Figure 7.1. They indicate the signal source, the transmitter, the wireless channel, the receiver and the signal sink. Within every module, there exist sub-modules to split the task into several sub-tasks and have them accomplished separately by the models, for example, *BPU_T* in *TX* calls *scrambler*, *channel_coder* and *interleaver* to deal with all bit processing tasks. Alternatively, modules can call models directly to

[1] LiLaS is descent from the Software-Defined-Radio Workbench (SDR-WB) [67, 68].

handle the basic signal processing. For example, *msource* in *SOURCE* generates random data bits to be transmitted.

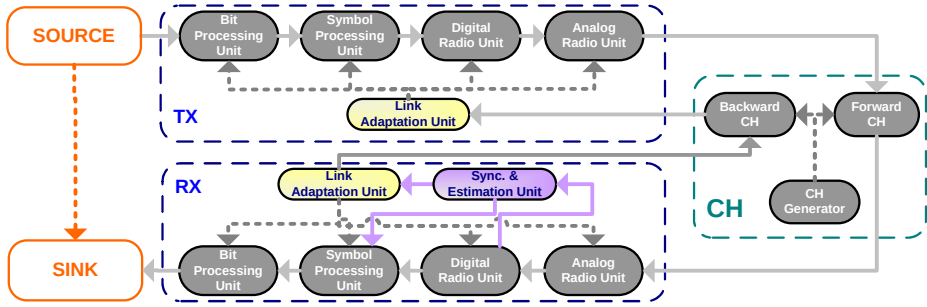

Figure 7.1: *Block diagram of the modularized simulator.*

Modules

The *SOURCE* generates data bits that are to be transmitted. Then the data bits are encoded and mapped into symbols in the *TX* before they are sent to the antennas. Through *CH*, the discrete-time signal is received at the *RX*, where the data bits are detected. The results such as BER and spectral efficiency are computed and shown in the *SINK*, both in table and graphical format.

The *TX* and *RX* consist of several generic sub-modules: *BPU* for the Bit Processing Unit, *SPU* for the Symbol Processing Unit, *DRU* for the Digital Radio Unit, *ARU* for the Analog Radio Unit, *SEU* for the Synchronization and Estimation Unit, and *LAU* for the Link Adaptation Unit, which is dedicated for adaptation techniques as discussed in previous chapters.

The *CH* is made up of three sub-modules: *GCH* to generate the complex valued channel matrix, *FCH* to feed the transmitted signal through the channel generated by *GCH*, *RCH* to feedback CSI from *RX* to *TX*, which is used in adaptive systems. To generate various types of channel, e.g., i.i.d. Rayleigh fading channels and Ricean channels, *GCH* employs different channel generating models.

Sub-Modules

Since *TX* and *RX* have complicated signal processing procedures, it is necessary to divide them into sub-procedures that are treated separately by sub-modules. *BPU_T* include all the bit processing units, like data bit scrambler, convolutional channel coding and block interleaver. *SPU_T* deals with the symbol processing part. It maps the bits into symbols and operates some application-specific functions, like MIMO encoding. *DRU_T* is comprised of the blocks that are located before the DA-converter, such as OFDM modulation, interpolation and channel

filtering. ARU_T include the DA-converter, frequency translation, power amplifier, and transmitter filter. At the receiver, there exist corresponding models to the transmitter in reverse order. Besides, there is a special sub-module, SEU_R, which takes care of channel synchronization and estimation. LAU_R deals with link adaptation that is invoked in adaptive systems. More specifically, it is responsible for making adaptation decisions based on the CSI. This could be done either at transmitter or at receiver.

Models and Instantiations

The models are the basic units that perform the signal processing to realize an atomic functionality. All of the models are parameterized to ease reconfiguration. The values of the parameters are pre-defined in a corresponding ini-file of the model, where they are systematically organized and can be easily altered.

It is not unusual that some models will be called by different sub-modules at different places. In that case, the model needs a specific ini-file for every occurrence. This situation can be addressed by instantiation. An instantiation of a model can be regarded as a shell of the model, with specific parameter values defined in the shell's ini-file.

The invocation of instantiations by a sub-module is shown in Figure 7.2, where the sub-module has to call different models in different application cases. In case of APP1, model a and b are called in order, where model a has two instantiations, denoted as a1 and a2, and model b has one instantiation. If APP2 is the case, instantiations x and y are to be employed, based on the original model x and y, respectively. The settings of the models and instantiations in every ini-file are carried out manually, depending on the specific designs. On the other hand, we don't need to hardcode any models name within the sub-module m-file. Instead, the sub-module automatically searches for the models' name and order that are to be called in the sub-module ini-file.

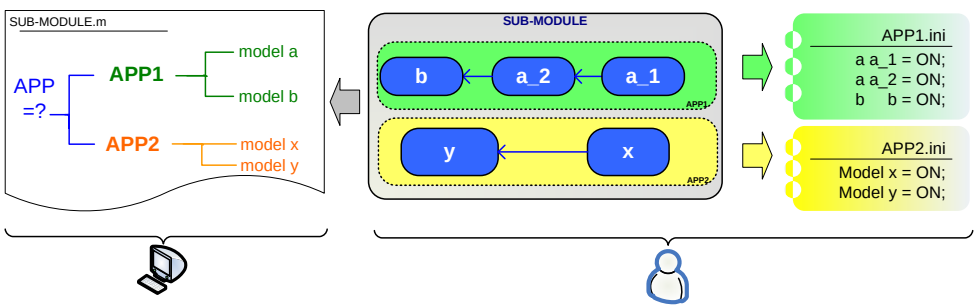

Figure 7.2: *Illustration of sub-module design.*

Other Functions

Besides the kernel, modules, sub-modules and models functions, there are other supporting functions. For instance, readParam.m helps each module/model to read in the parameter values set in the ini-file.

7.2 Control Flows

The data flows supported by LiLaS can be categorized into two modes, channel-adaptive mode and non-adaptive mode, which correspond to adaptive transmission and non-adaptive transmission, respectively.

- Adaptive mode deals with adaptive transmission that adjusts the transmission parameters such as rate and power depending on CSI. Figure 7.3 shows the control flow in the "Run" phase. As the transmission starts, CH is called to generate channel response samples, $\mathbf{H}$, according to the selected channel model. Channel estimation is carried out with the assistance of training sequences. Based on the estimated channel, $\hat{\mathbf{H}}$, the channel quality is to be identified. If bad channel quality is detected, a new channel realization is generated and followed by the same route as described above. If the channel quality is good, the best suited transmission parameters are fed back to the transmitter. Data transmission is initiated based on the feedback information. We assume the channel remains unchanged, thereby the same channel realization $\mathbf{H}$ is to be used. At the receiver, the estimated channel from the previous estimation, $\hat{\mathbf{H}}$, is employed for detection. In Monte-Carlo simulation, the transmission only stops when the loop is finished.

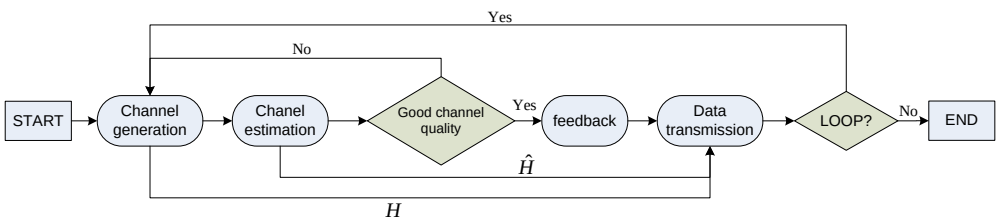

Figure 7.3: *Data flow of channel-adaptive transmissions.*

- Non-adaptive mode does not have CSI at the transmitter and the transmission parameters are fixed regardless of the variation of the wireless channel. As illustrated in Figure 7.4, the procedure is similar to the case of adaptive transmission except that the channel quality control is not included in this case.

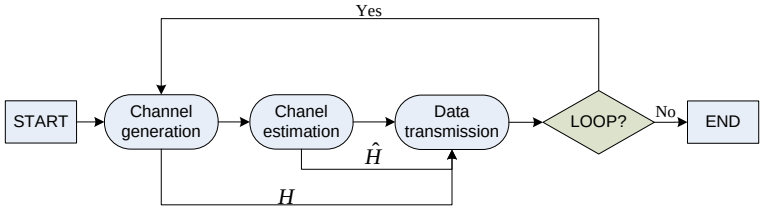

Figure 7.4: *Data flow of non-adaptive transmissions.*

7.3 File Structure

The main file structure of the simulator is illustrated in Figure 7.5. All m-files and ini-files are located in categorized folders under the main directory LiLaS. There exist two files on the first level, LiLaS.m and LiLaS.ini, which are the main function and it's corresponding ini-file that contains the system parameters. LiLaS.m call phase functions that are placed under the directory of KERNEL, such as Init.m, Setup.m, Run.m, and Wrapup.m. Depending on the transmission mode, adaptive or non-adaptive, different versions of Run.m are called to execute the data flow as defined in Figure 7.3 or Figure 7.4. Within every phase, module and sub-module files, located under the directory of MODULES, are called in a certain order according to the desired data flow. These files and directories mentioned above define the architecture and data path of the simulator, which are unaccessible to users. On the other hand, there are user accessible directories, where the files can be visited and altered by the users themselves, e.g., TEMPLATE, APPS, RESULTS, LIB, and sub-directories under them. TEMPLATE contains the template files for writing user-specific models and parameter files. Various transmission schemes are specified in APPS. For example, all parameters related to MIMO-SVD are placed in a sub-folder named *MIMO-SVD*. The parameters tell the simulator which models should be invoked in which sub-module or module, as shown in Figure 7.2. Simulation results are collected in the directory of *RESULTS*. *LIB* includes all models and supporting files. Users can build up their own models under this directory.

7.4 Case Study

Thus far, the transmission schemes that can be implemented by LiLaS include: SISO, MIMO, OFDM, MIMO-OFDM, offset-QAM, and DS-CDMA. Various algorithms are available for MIMO/MIMO-OFDM schemes, e.g., SVD, OSTBC, D-STTD [54], Beamforming, ZF, and MMSE. In this section, we present an example of simulation results for MIMO-OFDM systems using LiLaS.

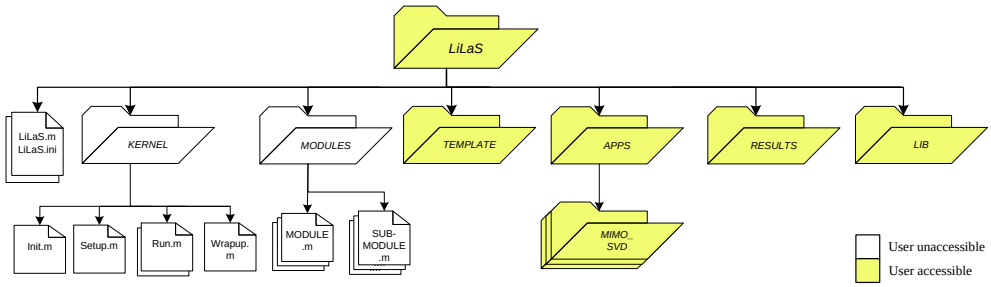

Figure 7.5: *File structure of the simulator.*

MIMO-OFDM

There are four transmit antennas and four receive antennas, the number of sub-carriers for OFDM is 64, 48 out of which are used to carry the information-bearing signals. We assume a frequency-selective Rayleigh fading channel generated by a deterministic spatial-temporal channel model [63]. Perfect CSI is available at the transmitter so that adaptive modulation is applied for every scalar channel.

- **Setup**
  In the setup phase, the system parameters are read from MIMOOFDM-SVD.ini, an application-specific ini-file. Then the simulator goes through all sub-modules that are to be invoked later in the run phase to initialize the parameters.

- **Run**
  Scenario_CSIT is called by *Run* to control the data flows, as can be seen in Figure 7.3. To get statistical results, we run Monte-Carlo simulations with 30 channel realizations.

- **Wrapup**
  The average bit-loading for all 48 sub-carriers are presented graphically in Figure 7.6, in which the bit-loading for the 1st and 2nd sub-channels (created by SVD) are shown, respectively.

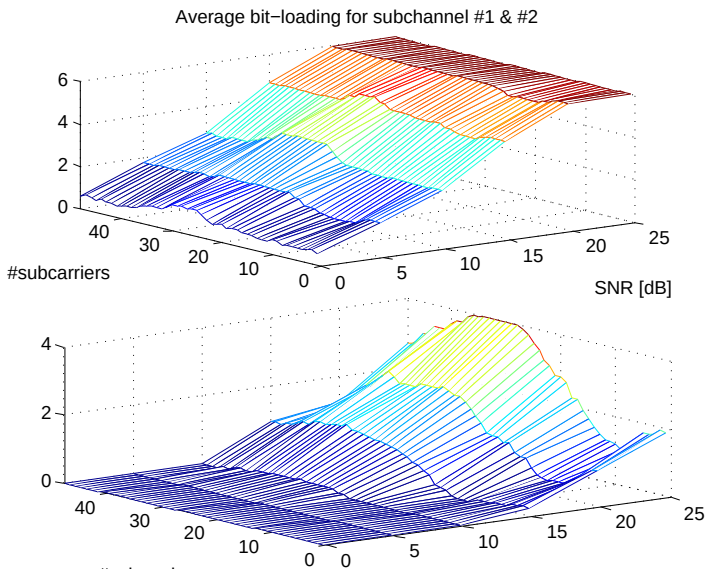

Figure 7.6: *Number of bits loaded on sub-carriers.*

Chapter 8

Conclusions and Future Work

8.1 Conclusions

In this dissertation, we investigated adaptive transmission strategies to maximize the spectral efficiency for multiple antenna systems. Our particular focus was on the performance that can be achieved by using adaptive modulation and adaptive power allocation techniques.

We began our investigation with adaptive modulation schemes that satisfy an I-BER constraint or an A-BER constraint. The closed-form expressions for the average spectral efficiency and BER were provided, based on which the problem of A-BER constraint is solved. It was shown that the A-BER constraint is able to achieve higher average spectral efficiency with prohibitive computational complexity. To reach similar performance as the A-BER constraint at the cost of relatively low complexity, we thereby proposed a nonlinear optimization method, namely the Levenberg-Marquardt (LM) algorithm. With the LM algorithm, only one set of SNR thresholds were used over the whole SNR region.

The adaptive modulation schemes were applied to various MIMO coding schemes, e.g., SVD, Beamforming, OSTBC, ZF, and MMSE. The closed-form solutions for the average spectral efficiency were obtained for each scheme based on the p.d.f. of the effective SNR. Furthermore, distinct average spectral efficiencies were manifested by using different MIMO schemes. This led to the exploration of the optimal MIMO coding scheme that achieves the highest average spectral efficiency.

As we extended the adaptation to include variable transmit power, the performance could be further boosted by adjusting the transmit power to channel quality accordingly. In case of OSTBC, a Truncated Channel Inversion (TCI)-like power strategy was applied to ensure that instant error probability meet the target BER, i.e., I-BER constraint. The optimal SNR thresholds were chosen to fulfill the average power constraint. When SVD is concerned, a practical power allocation policy subject to a peak power constraint and an I-BER constraint was proposed, referred to as greedy power allocation. This scheme can achieve comparable performance

to the optimal exhaustive search scheme with much less complexity.

The impact of imperfect channel estimation on the performance was studied for adaptive modulation and adaptive power allocation systems. The adaptation schemes were tailored to tolerate the interferences caused by estimation error, but it resulted in saturation of the average spectral efficiency as SNR increases.

Last but not the least, a reconfigurable versatile simulator that accommodates a variety of transmission schemes was described. The simulator has a hierarchical structure consisting of generic blocks and each block is parameterized for ease of reconfiguration.

8.2 Future Work

A straightforward task is to obtain the optimal average spectral efficiencies for other MIMO algorithms by imposing the A-BER constraint or the LM algorithm. If power allocation is considered, we can even achieve higher performance. Another possible improvement can be achieved by using channel coding. Furthermore, the concept of average spectral efficiency can be employed in cross-layer design problems to provide more accurate estimation of the performance.

The main functionalities of the simulator LiLaS have already been finished, but more channel models are needed, such as the channel model for 802.11n or real channel data. To cope with the cross-layer design, simple MAC layer and network layer will be incorporated to take into account the problems of higher layers. For efficiency purposes, the channel coding/decoding based on C/C++ should be added. Finally, implementation of LiLaS in hardware with special focus on adaptation strategies is of great interest. FPGA is a promising candidate to implement the baseband signal processing in the digital domain. The simulator will find applications in product testing, where it can provide input signals to the device under test (DUT) and collect the output signals for evaluation.

Bibliography

[1] I. E. Telatar, "Capacity of multi-antenna gaussian channels", *European Transactions on Telecommunications*, vol. 10, Nov.-Dec. 1999.

[2] G. J. Foschini, "Layered space-time architecture for wireless communication in a fading environment when using multi-element antenna", *Bell Labs Technical Journal*, vol. 1, no. 2, pp. 41-59, 1996.

[3] G. J. Foschini and M. J. Gans, "On limits of wireless communications in a fading environment when using multiple antennas ", *Wireless Personal Communications*, no. 6, pp. 315-335, 1998.

[4] S.M. Alamouti, "A simple transmit diversity technique for wireless communications", *IEEE Journal on Selected Areas in Communications*, vol. 16, no. 8, Oct. 1998.

[5] V. Tarokh; H. Jafarkhani; A. R. Calderbank, "Space-time block codes from orthogonal designs", *IEEE Transactions on Information Theory*, vol. 45, no. 5, pp. 1456-1467, July 1999.

[6] D. Gerlach and A. Paulraj, "Adaptive transmitting antenna arrays with feedback", *IEEE Signal Processing Letters*, vol. 1, no. 10, pp. 150-152, Oct. 1994.

[7] Da-Shan Shiu and M. Kahn, "Layered space-time codes for wireless communications using multiple transmit antennas," in *Proc. IEEE International Conference on Communications,* pp. 436-440, 1999.

[8] A. Goldsmith; S. A. Jafar; N. Jindal; S. Vishwanath, "Capacity limits of MIMO channels," *IEEE Journal on Selected Areas in Communications,* vol. 21, no. 5, pp. 684-702, June 2003.

[9] J. F. Hayes, "Adaptive feedback communications," *IEEE Transactions on Communications,* vol. COM-16, pp. 29-34, Feb. 1968

[10] A. J. Goldsmith and S. G. Chua, "Variable-rate variable-power MQAM for fading channels," *IEEE Transactions on Communications*, vol. 45, no.10, pp. 1218-1230, Oct. 1997.

[11] H. Matsuoka, S. Sampei, N. Morinaga and Y. Kamio, "Symbol rate and modulation level controlled adaptive modulation/TDMA/TDD for personal communication systems," in *Proc. IEEE Vehicular Technology Conference*, pp. 487-491, Apr. 1996.

[12] S. M. Alouini and A. J. Goldsmith, "Adaptive Modulation over Nakagami Fading Channels," *J. Wireless Commun.*, vol. 13, no. 1-2, pp. 119-143, May 2000.

[13] S. T. Chung and A. J. Goldsmith, "Degrees of freedom in adaptive modulation: a unified view," *IEEE Transactions on Communications*, vol. 49, no.9, pp. 1561-1571, Sep. 2001.

[14] A. Maaref and S. Aissa, "Rate-adaptive M-QAM in MIMO diversity systems using space-time block codes," in *Proc. IEEE PIMRC 2004*, vol. 4, pp. 2294-2298, Sep. 2004.

[15] B. Holter, G. E. Oien, K. J. Hole and H. Holm, "Limitations in spectral efficiency of a rate-adaptive MIMO system utilizing pilot-aided channel prediction," in *Proc. IEEE Vehicular Technology Conference*, pp. 282-286, Apr. 2003.

[16] Z. Zhou, B. Vucetic, M. Dohler and Y. H. Li, "MIMO systems with adaptive modulation," *IEEE Transactions on Vehicular Technology*, vol. 54, no. 5, pp. 1828-1842, Sept. 2005.

[17] X. Zhang and B. Ottersten, "Power Allocation and Bit Loading for Spatial Multiplexing in MIMO Systems," In *Proc. IEEE International Conference on Acoustics, Speech, and Signal Processing*, April, 2003.

[18] S. T. Chung, A. Lozano and H. C. Huang, "Low complexity algorithm for rate and power quantization in extended V-BLAST," in *Proc. IEEE Vehicular Technology Conference*, pp. 910-914, 2001.

[19] W. J. Choi, K. W. Cheong and J. M. Cioffi, "Adaptive modulation with limited peak power for fading channels," In *Proc. IEEE Vehicular Technology Conference*, 2000.

[20] P. F. Xia; S. L. Zhou; G. B. Giannakis, "Adaptive MIMO-OFDM based on partial channel state information," *IEEE Transactions on Signal Processing*, vol. 52, no. 1, Jan. 2004.

[21] Mattias. Wennström, "On MIMO Systems and Adaptive Arrays for Wireless Communications, Analysis and Practical Aspects", *Ph.D. thesis*, Signal and Systems, Uppsala University, 2002.

[22] J. Ham, S. Shim, K. Kim, and C. Lee, "A simplified adaptive modulation scheme for D-STTD systems with linear receivers," *IEEE Communication Letters* vol. 9, no. 12, pp. 1049-1051, Dec. 2005.

[23] L. Fan, C. He, Z. Wang and X. Che, "Transmit power and bit allocation for the MIMO system," in *Proc. IEEE Global Telecommunications Conference*, 2005.

[24] H. Shi; T. ABE; H. SUDA, "Iterative power allocation scheme for MIMO systems," *IEICE Transactions on Communications*, vol. e89-b, no. 3, pp. 791-800, Mar. 2006.

[25] J. L. Huang and S. Signell, "The Application of Rate Adaptation with Finite Alphabet in MIMO-OFDM," in *Proc. IEEE International Conference on Information, Communications and Signal Processing, 2005,* pp. 946-949, Dec. 2005.

[26] J. L. Huang and S. Signell, "Discrete Rate Spectral Efficiency Improvement by Scheme Switching for MIMO Systems," in *Proc. IEEE International Conference on Communications 2008,* pp. 3998-4002, May 2008.

[27] J. L. Huang and S. Signell, "On Performance of Adaptive Modulation in MIMO Systems Using Orthogonal Space-Time Block Codes", second submission to *IEEE Transactions on Vehicular Technology.*

[28] Z. Y. Wang and C. He, "Adaptive modulation MIMO system based on minimizing transmission power," *Journal Zhejiang University Science A,* pp. 1046-1050, 2006.

[29] C. S. Park and K. B. Lee, "Transmit Power Allocation for BER Performance Improvement in Multicarrier Systems," *IEEE Transactions on Communications,* vol. 52, no. 10, pp. 1658-1663, Oct. 2004.

[30] E. Biglieri and G. Taricco, *Transmission And Reception With Multiple Antennas: Theoretical Foundations*, Now Publishers, 2004.

[31] H. Vikalo, B. Hassibi and T. Kailath, "Iterative decoding for MIMO channels via modified sphere decoder," *IEEE Transactions on Wireless Communications,* vol. 3, no. 6, Nov. 2004.

[32] V. Tarokh, N. Seshadri and A. R. Calderbank, "Space-time codes for high data rate wireless communication: Performance analysis and code construction," *IEEE Transactions on Information Theory*, vol. 44, pp. 744-765, Mar. 1998.

[33] H. Bölcskei and A. J. Paulraj, "Space-frequency coded broadband OFDM system," in *Proc. IEEE Wireless Communications and Networking Conference 2000*, vol. 1, pp. 1-6, Sept. 2000.

[34] David Tse, Pramod Viswanath, *Fundamentals of Wireless Communication*, Cambridge University Press, 2005.

[35] L. Zheng and D. Tse, "Diversity and Multiplexing: A Fundamental Tradeoff in Multiple Antenna Channels", *IEEE Transactions on Information Theory,* vol. 49(5), May 2003.

[36] G. G. Raleigh and J. M. Cioffi, "Spatio-temporal coding for wireless communication", *IEEE Transactions on Communications*, vol. 46, no. 3, pp. 357-366, March 1998.

[37] A. M. Wyglinski; F. Labeau; P. Kabal, "An efficient bit allocation algorithm for multicarrier modulation," in *Proc. IEEE Wireless Communications and Networking Conference*, pp. 1194-1199, March 2004.

[38] Andrea Goldsmith, *Wireless Communications*, Cambridge University Press, 2005.

[39] Roger A. Horn and Charles R. Johnson, *Matrix Analysis,* Cambridge University Press, 1999.

[40] D. A. Gore; R. W. Jr. Heath; A. J. Paulraj, "Transmit selection in spatial multiplexing systems," *IEEE Communication Letters*, vol. 6, no. 11, pp. 491-493, Nov. 2002.

[41] Da-Shan Shiu; G. J. Foschini; M. J. Gans; J. M. Kahn, "Fading correlation and its effect on the capacity of multielement antenna systems," *IEEE Transactions on Communications,* vol. 48, no. 3, pp. 502-513, March 2000.

[42] P. Li; D. Paul; R. Narasimhan; J. Cioffi, "On the distribution of SINR for the MMSE MIMO receiver and performance analysis," IEEE Transactions on Information Theory, vol.52, no.1, pp.271-286, Jan. 2006.

[43] K. Madsen, H. B. Nielsen, O. Tingleff, *Methods for non-linear least squares problems*, 2nd Edition, Technical University of Denmark, April, 2004.

[44] W. H. Press; B. P. Flannery; S. A. Teukolsky; W. T. Vetterling, *Numerical Recipes in C: The Art of Scientific Computing*, Cambridge University Press, 1992.

[45] J. L. Huang and S. Signell, "On Spectral Efficiency of Low-Complexity Adaptive MIMO Systems in Rayleigh Fading Channel," to appear in *IEEE Transactions on Wireless Communications.*

[46] Qingwen Liu; Shengli Zhou; G. B. Giannakis, "Cross-Layer combining of adaptive Modulation and coding with truncated ARQ over wireless links," *IEEE Transactions on Wireless Communications* , vol. 3, no. 5, pp. 1746-1755, Sept. 2004.

[47] K. J. Hole; H. Holm; G. E. Oien, "Adaptive multidimensional coded modulation over flat fading channels," *IEEE Journal on Selected Areas in Communications* , vol. 18, no. 7, pp. 1153-1158, Jul. 2000.

[48] A. J. Goldsmith; S. G. Chua, "Adaptive coded modulation for fading channels," *IEEE Transactions on Communications* , vol. 46, no. 5, pp. 595-602, May 1998.

[49] S. Sanayei; A. Nosratinia, "Antenna selection in MIMO systems," *IEEE Communications Magazine* , vol. 42, no. 10, pp. 68-73, Oct. 2004

[50] Zhuo Chen; I. B. Collings; Zhendong Zhou; B. Vucetic, "Novel Transmit Antenna Selection Schemes with Reduced Channel Feedback Rate Requirement," in *Proc. IEEE Personal, Indoor and Mobile Radio Communications,* pp. 1-5, Sept. 2007.

[51] A. J. Goldsmith and P. P. Varaiya, "Capacity of fading channels with channel side information," *IEEE Transactions on Information Theory*, vol. 43, no. 6, pp. 1986-1992, Nov. 1997.

[52] J. L. Huang and S. Signell, "A Novel Power Allocation Strategy for Finite Alphabet in MIMO Systems," in *Proc. IEEE Vehicular Technology Conference*, Melbourne, May, 2006.

[53] A. Lozano; A. M. Tulino and S. Verdu, "Mercury/waterfilling: optimum power allocation with arbitrary input constellations," in *Proc. IEEE International Symposium Information Theory,* Sept. 2005.

[54] Texas Instruments. "Double-STTD scheme for HSDPA systems with four transmit antennas: link level simulation results", *TSG-R, WG1 document, TSGP1 20(01)0458*, May 2001, Busan, Korea.

[55] Richard Van Nee, Ramjee Prasad, *OFDM For Wireless Multimedia Communications*, Artech House Publishers, 2000.

[56] G. L. Stüber; J. R. Barry; S. W. McLaughlin; Y. Li; M. A. Ingram and T. G. Pratt; "Broadband MIMO-OFDM wireless communications",*Proceedings of the IEEE* , vol. 92, pp. 271-294, Feb. 2004.

[57] R. H. Clarke, "A statistical theory of mobile-radio reception," *Bell System Technical Journal,* vol. 47, pp. 957-1000, 1968.

[58] Technical specification group radio access network, "Spatial channel model for multiple input multiple output (MIMO) simulations (release 6)," *Technical report 3GPP TR25.996 V6.1.0,* 3rd Generation partnership project, Sept. 2003.

[59] J. G. Proakis, *Digital Communications*, Fourth Edition, McGraw-Hill Higher Education, 2001

[60] G. L. Stüber, *Principles of Mobile Communications*, Kluwer Academic Publishers, 2000.

[61] K. Yu, "Multiple input multiple output radio propagation channels: charateristics and models," *Ph.D. thesis,* Royal Institute of Technology, Stockholm, Sweden, 2005.

[62] D. Chizhik; F. Rashid-Farrokhi; J. Ling; A. Lozano, "Effect of antenna separation on the capacity of BLAST in correlated channels," *IEEE Communications Letters*, vol. 4, no. 11, pp. 337-339, Nov 2000.

[63] Jinliang Huang, *A Matlab/Octave simulation environment for SDR with application to OFDM and MIMO*, Master thesis, ICT/ECS, Royal Institute of Technology, Stockholm, Sweden, Feb. 2005.

[64] D. Gesbert; M. Shafi; D.S. Shiu; P. J. Smith and A. Naguib, "From Theory to Practice: An Overview of MIMO Space-Time Coded Wireless Systems", *IEEE Journal on Selected Areas in Communications*, vol. 21, no. 3, pp. 281-302, Apr. 2003.

[65] R. G. Gallager, *Information theory and reliable communication.* New York: John Wiley and Sons, 1968.

[66] C. M. Grinstead and J. L. Snell, *Introduction to probability*, American Mathematical Society, 1997.

[67] S. Signell and J. L. Huang, "A Matlab/Octave simulation workbench for software defined radio," In *Proc. IEEE Norchip*, Linköping, Sweden, November 2006.

[68] S. Signell and J. L. Huang, "A Simulation Environment for Multi-Antenna Software Defined Radio", In *Proc. IEEE ICICS,* Singapore, December 2007.

[69] S. Zhou and G. B. Giannakis, "How accurate channel prediction needs to be for transmit-beamforming with adaptive modulation over Rayleigh MIMO channels," *IEEE Transactions on Wireless Communications*, vol. 3, no. 4, pp. 1285-1294, July 2004.

[70] R. W. Heath, and A. J. Paulraj, "Switching between diversity and multiplexing in MIMO systems," *IEEE Transactions on Communications*, vol.53, no.6, pp. 962-968, Jun. 2005.

[71] S. Catreux; V. Erceg; D. Gesbert; W. Heath Jr., "Adaptive modulation and MIMO coding for broadband wireless datanetworks," *IEEE Communications Magazine*, vol. 2, pp. 108-115, Jun. 2002.

[72] A. Forenza; M. R. McKay; I. B. Collings and R. W. Heath Jr, "Switching between OSTBC and spatial multiplexing with linear receivers in spatially correlated MIMO channels," in *Proc. IEEE Vehicular Technology Conference*, May 2006.

[73] J. L. Huang and S. Signell, "Adaptive MIMO Systems in 2×2 Uncorrelated Rayleigh Fading Channel," in *Proc. IEEE Wireless Communications and Networking Conference*, Mar. 2007.

[74] T. Weber; A. Sklavos and M. Meurer, "Imperfect channel-state information in MIMO transmission," *IEEE Transactions on Communications*, vol.54, no.3, pp. 543-552, March 2006